

Auxin, Actin, and Polar Patterning in Tobacco Cells

(Nicotiana tabacum L. cv. Bright Yellow 2)

Zur Erlangung des akademischen Grades eines

DOKTORS DER NATURWISSENSCHAFTEN

(Dr. rer. nat.)

der Fakultät für Chemie und Biowissenschaften der
Universität Karlsruhe (TH)
vorgelegte

DISSERTATION

von

Jan Maisch

aus Karlsruhe

Dekan: Prof. Dr. H. Puchta
Referent: Prof. Dr. P. Nick
Korreferent: Prof. Dr. M. Bastmeyer
Tag der mündlichen Prüfung: 14. Februar 2007

Die vorliegende Dissertation wurde am Botanischen Institut der Universität Karlsruhe (TH), Lehrstuhl 1 – Molekulare Zellbiologie, im Zeitraum von Dezember 2003 bis Dezember 2006 angefertigt.

Mein besonderer Dank gilt Herrn Prof. Dr. Peter Nick für die hervorragende Betreuung der Doktorarbeit und das in mich gesetzte Vertrauen.

Herrn Prof. Dr. Martin Bastmeyer danke ich für die Übernahme des Korreferats.

Frau Dr. Christina Süßlin und Frau Dr. Petra Hohenberger ermöglichten mir den reibungslosen Einstieg in molekularbiologische Arbeitstechniken.

Frau Sabine Purper danke ich für die Unterstützung in allen Bereichen der pflanzlichen Zellkultur und Herrn Kai Eggenberger für die Korrektur zahlreicher Manuskripte.

Ferner will ich mich bei allen Mitarbeitern des Botanischen Instituts I für die angenehme Arbeitsatmosphäre bedanken.

Meine Arbeit wurde finanziell durch ein Stipendium der Landesgraduiertenförderung Baden-Württemberg und durch Mittel der Deutschen Forschungsgemeinschaft bzw. des Deutschen Akademischen Austauschdienstes unterstützt.

Zusammenfassung

Der polare Transport des Phytohormons Auxin ist für Polarität und Musterbildung zentral. Auf zellulärer Ebene zeigt sich diese Polarität als Gradient von Auxin-Efflux-Komponenten (den PIN-Proteinen). Dieser Gradient entsteht über Actomyosin-abhängigen Vesikelfluss.

Die Dissertation beschäftigt sich mit der Frage, welchen Einfluss die Organisation der Actinfilamente auf den Auxintransport hat. Um die Polarität des Auxinflusses im physiologischen Zusammenhang verfolgen zu können, wurden Teilungsmuster in der Tabakzelllinie BY-2 (*Nicotiana tabacum* L. cv. Bright Yellow 2) untersucht. Innerhalb eines Zellfadens sind die Zellteilungen teilweise synchron. Hemmstoffe des polaren Auxintransports stören diese Synchronisierung. Daher konnte der Synchronisierungsgrad der Zellteilungen als physiologischer Anzeiger für die Effizienz des polaren Auxintransports benutzt werden.

Durch die Überexpression des Actinbinde-Proteins Talin wurde eine stark gebündelte Actinkonfiguration hervorgerufen, welche die Synchronisierung der Zellteilungen beeinträchtigte. Die Zugabe von Auxinen, die polar transportiert werden, stellte sowohl die normale Actinorganisation als auch die Synchronisierung der Zellteilungen wieder her. Daher kontrolliert Auxin vermutlich in einer selbstverstärkenden Rückkopplungsschleife seinen eigenen polaren Transport über Veränderung der Actinkonfiguration.

Um die Rolle der Mikrofilamentpolarität während der Entstehung von Zellpolarität zu untersuchen, wurden mittels eines Fusionskonstruktes (RFP-ARP3) Actinnukleationsstellen *in vivo* sichtbar gemacht, die in den Spitzen von terminalen Tabakzellen gehäuft auftraten. Die Verteilung dieser Nukleationsorte wurde im Vergleich mit der Auxin-Efflux-Komponente PIN1 im Verlauf der geordneten Zellteilung untersucht. Dies führte zu einem Modell der Musterbildung, das Auxintransport, Actincytoskelett und Zellpolarität verknüpft. Nach diesem Modell ist der in den terminalen Zellen beobachtete Gradient der Actinnukleationsorte an der Wiederherstellung des polaren Auxinflusses beteiligt, der die Teilung der Tochterzellen synchronisieren wird.

Table of Contents

1. Introduction	1
1.1 What is a pattern and how is it brought about in plants?	1
1.2 Pattern formation depends on cell polarity	3
1.3 Auxin canalisation.....	5
1.4 Polar auxin transport is mediated by polarly localised efflux carriers.....	7
1.5 Components of the auxin-transport machinery	9
1.5.1 <i>Pin-formed</i> proteins	9
1.5.2 Targeted vesicle flow ensures the polar localisation of auxin-efflux carriers	10
1.5.3 Actin assists the polar targeting of the auxin-efflux complex.....	11
1.5.4 The ARP2/3 complex nucleates actin polymerisation in a polarly and spatially controlled manner.....	13
1.6 Scope of the dissertation	14
1.7 The tobacco cell line BY-2 as a model system for auxin-dependent, supracellular patterning of cell divisions	16
2. Materials and Methods.....	18
2.1 Tobacco cell cultures	18
2.2 Constructs	19
2.2.1 <i>pVKH18En6-YFP-talin</i> construct	19
2.2.2 <i>pK7WGF2-FABD2</i> construct	19
2.2.3 <i>p2GWR7-ARP3</i> construct	20
2.3 <i>In silico</i> analysis.....	20
2.4 Transformation and establishment of tobacco BY-2 cells	21
2.4.1 Biolistic, stable expression of YFP-mT	21
2.4.2 Biolistic, transient expression of RFP-ARP3	22
2.4.3 <i>Agrobacterium</i> -mediated, stable expression of GFP-FABD2	22
2.5 Phyto tropin and auxin treatments	23
2.6 Latrunculin B treatment, cold treatment, and recovery experiments.....	23

2.7	Visualisation of actin filaments by rhodamine-phalloidin staining	24
2.8	Quantification of pattern and morphology	24
2.8.1	Determination of frequency distributions and cell elongation	24
2.8.2	Determination of cell viability and cell density	25
2.8.3	Determination of mitotic indices	25
2.8.4	Quantification of ARP3-expression patterns.....	26
2.9	Microscopy and image analysis.....	26
3.	Results	28
3.1	The impact of actin organisation on patterned cell division in BY-2 cell files	28
3.1.1	Cell division within cell files of BY-2 is synchronised by a NPA-sensitive signal.....	28
3.1.2	The actin filaments are constitutively bundled in a BY-2 cell line overexpressing YFP-talin	34
3.1.3	The synchrony of cell division is affected by bundling of actin	38
3.1.4	The synchrony of cell division can be restored by polar transportable auxins.....	40
3.2	Localisation of the actin-nucleation factor ARP3	42
3.2.1	Isolation of tobacco ARP3	42
3.2.2	Visualisation of actin filaments by stable GFP-fimbrin expression ..	45
3.2.3	Localisation of actin-nucleation sites upon transient expression of RFP-ARP3 in BY-2 GFP-FABD2 cells.....	47
3.2.4	ARP3 is enriched in the distal halves of terminal cells	49
3.2.5	Behaviour of ARP3 and PIN1 during divisional patterning	51
3.3	Summary	54
4.	Discussion	55
4.1	Actin is involved in auxin-dependent patterning.....	55
4.1.1	Auxin synchronises cell divisions in BY-2 cells	55
4.1.2	Generation of constitutively bundled actin by overexpression of mouse talin.....	56
4.1.3	Actin bundling impairs the auxin-dependent synchrony	57

4.1.4 Polarly transportable auxins restore the synchrony of the division pattern	58
4.1.5 Auxin controls its own transport by modulating the organisation of actin filaments	59
4.2 What controls the asymmetric cycling of the auxin-efflux carrier?	60
4.2.1 Actin organisation and directional auxin flow.....	61
4.2.2 A model on actin polarity and auxin fluxes during polar patterning...	62
4.3 Conclusion.....	67
4.4 Outlook	68
5. Acknowledgments.....	71
6. References	72
7. Appendix	83

List of Abbreviations

2,4-D	2,4-dichlorophenoxyacetic acid
ARFs	ADP-ribosylation factors
ARP3	actin-related protein 3
BFA	Brefeldin A
BY-2	tobacco cell line <i>Nicotiana tabacum</i> L. cv. Bright Yellow 2
FABD2	fimbrin actin-binding domain 2
GEFs	guanine nucleotide exchange factors
GFP	green fluorescent protein
IAA	indole-3-acetic acid
LatB	Latrunculin B
mT	mouse talin
NAA	1-naphthaleneacetic acid
NPA	1- <i>N</i> -naphthylphthalamic acid
PIN1	<i>pin-formed</i> protein 1
RFP	red fluorescent protein
ROPs	Rho-related GTPases of plants
SE	standard error
TIBA	2,3,5-triiodobenzoic acid
YFP	yellow fluorescent protein

1. Introduction

1.1 What is a pattern and how is it brought about in plants?

Form and shape represent the outstanding features of living organisms. Although organisms are complex, their various parts bear predictable, repeated relations to one another. It is this regularity, or the deviation from a random distribution of the various parts, referred to as a pattern, indicating that a shape emerges on the level of the whole. The regularity of form is characteristic not only for external shape and the microscopic arrangement of the various types of cells and tissues, it is also characteristic for the subcellular and molecular mechanisms proceeding within cells. Furthermore, patterns can emerge on the temporal as well as the spatial level.

Biological form is always the result of a non-random distribution of developmental processes. The removal of one part of a given organism changes the developmental fate of the remaining parts. Moreover, grafting embryonic tissues to ectopic locations can change developmental fate or induce the differentiation of neighbouring regions (Spemann, 1938). These general facts, demonstrated for plants more than 110 years ago (Vöchting, 1892), show that the developmental fate of a cell or tissue is flexible and depends on its location. It can be influenced by signals from other parts of the organism (Bünning, 1965). Thus, development involves spatial correlations over various distances including correlative interaction between neighbouring cells.

Plant development poses a special challenge to adaptation. In contrast to animals, plants are bound to their rooted positions. To compensate for this sessile lifestyle, plants have evolved an amazing capacity to adjust their development to environmental variability. As a consequence of this pronounced

developmental flexibility, plant morphogenesis is open and therefore characterised by indefinite growth. In addition, almost independently of its developmental history, each plant cell can reestablish a complete organism, referred to as somatic embryogenesis. The body plan of such somatic embryos is indistinguishable from those originating from normal, zygotic development. Generally, the principal totipotency of plant cells is difficult to reconcile with a pattern which has to be built into a preexisting spatial field. Thus, pattern formation in plants typically does not occur within a predetermined, limited population of elements, but in a situation where new elements are continuously added. Moreover, the patterning process has to work with elements that have a fixed position, because plant cells are usually permanently encased by surrounding walls which do not allow the cellular migration characteristic for animal development. Hence, morphogenetic changes in plants are exclusively brought about by flexible division and expansion of cells.

Thus, patterning in plants is based on iterative mechanisms which result from coordinative signals between the already defined (older) regions of the pattern and the newly formed elements of the field that still have to acquire a specific identity.

This implicates on the one hand that a pattern is partially derived from a vague pre-pattern, but must be continuously reinforced and perpetuated by ongoing patterning processes. Developmental information could be supplied by relatively simple pre-patterns, such as a gradient in the vicinity of an autocatalytic feedback loop of a signal. The demonstrations that simple chemical processes can yield a patterned distribution of products represented an important theoretical breakthrough in a deeper understanding of pattern formation. This type of mechanism can be described by the mathematics of reaction-diffusion systems that were adapted to biology (Turing, 1952) and have been used to model various biological patterns (foot-head patterning in *Hydra*, Gierer et al., 1972; segmentation in *Drosophila*, Meinhard, 1986; leaf venation, Meinhard, 1976). In these reaction-diffusion systems, a locally constrained, self-amplifying feedback loop of an activator is linked to a far-ranging mutual inhibition (Gierer and Meinhard, 1972).

On the other hand, patterning is brought about by communication between cells that exchange morphogenetic signals in a certain direction. In other words, patterning is driven by cell polarity. Therefore, synchrony and coordination between neighbouring cells are of extreme importance for the development of a functional tissue (Sachs, 1993).

1.2 Pattern formation depends on cell polarity

During investigations on the regeneration of new organs on branch cuttings, Vöchting (1878) uncovered the fundamental role of plant polarity for development. In his famous experiment (**Fig. 1**), he inverted a willow branch and observed that the roots and shoots emerged where they should, according to the former orientation of the branch, although the relation with gravity had changed. His conclusion was that these regenerative phenomena were not a mere response to an environmental factor, but demonstrated the innate polarity of the plant tissues themselves. He further inferred that each cell is polarised – analogous to a small magnet – and that the polarity of tissues is the sum of the polarities of its cells. Thus, axis and orientation are basic, essential expressions of a polar, patterned development.

Summarising the essence of Vöchting's experiment, plants are able to "remember" top and bottom, even if they are inverted. This memory of the original axis - referred to as polarity - can be traced down to a direction of each individual cell. Cell polarity is related to the directional flow of signals, such as the plant hormone auxin, and to the organisation of the cytoskeleton (actin, microtubules).

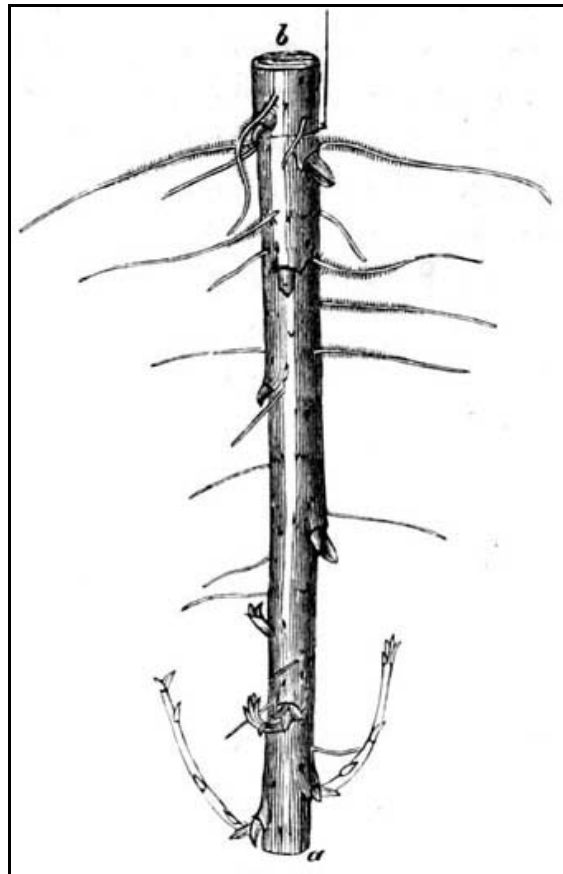


Figure 1: Evidence for a polarity of plant tissues. Cuttings taken along a willow branch all exhibit the same polar regeneration, even if the cuttings are kept inverted. Roots regenerate from the former base of a willow branch cutting (*b*), and bud growth occurs on its former apical side (*a*). From Vöchting (1878).

Within a plant tissue, the axis of a cell is intimately linked to the arrangement of cellulose microfibrils in the expanding cell wall, which in turn depends on an ordered array of cortical microtubules. The orientation of these microtubular arrays can be controlled through a panel of endogenous and environmental stimuli. Reorientation of cell expansion by directional cues is common in cells endowed with tip growth (such as pollen tubes or root hairs).

In addition, a key event for cell polarity is cell division, because it defines symmetry, axis and orientation of the new cell wall. Thus, cell division lays down the spatial constraints of subsequent cell growth.

Reorientations of cell division, mostly in combination with mitotic asymmetry, are often accompanied by the establishment of two alternative developmental

pathways for the daughter cells. This indicates a role in partitioning of signal molecules that influence cell fate. For example, asymmetric division is a common feature of zygotic development (for review see Jan and Jan, 2000). In the *gnom* mutant, where the first zygotic division is symmetric, the development fate of the descendant cells is dramatically altered resulting in embryos with defective apical-basal morphogenesis (Mayer et al., 1993). Asymmetric division also precedes differentiation of the stomatal guard cell pair from their protodermal precursors in the epidermis of plant leaves (for review, see Larkin et al., 1997). Asymmetric division is based on cell polarity which, in plants, is intimately linked to the directional transport of the plant hormone auxin.

1.3 Auxin canalisation

The morphogenetic role of auxin extends far beyond the generation of cell polarity. Auxin is used as a signal to coordinate the formation of patterns (for review, see Berleth and Sachs, 2001). Classical examples for auxin-dependent patterning have been the formation of leaf veins (Mattsson et al., 1999), the positioning of meristems (Reinhard et al., 2000), and the organisation of vascular tissue (Sachs, 2000).

The self-amplification of cell polarity by a polar auxin flow has been linked to directional intracellular traffic that contains positive feedback loops in combination with lateral inhibition resulting in an ordered pattern (for review, see Nick, 2006). This mechanism has been elegantly demonstrated for the formation of conductive tissues in wound healing of internodes or for the venation of developing leaves (Sachs, 2000) leading to the auxin-canalisation model (**Fig. 2**).

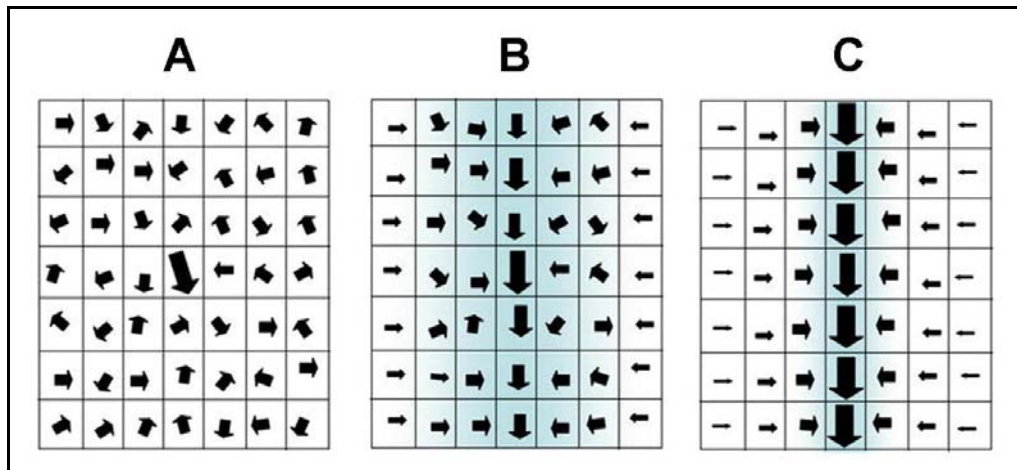


Figure 2: Formation of vascular bundles by auxin canalisation. The arrows indicate the direction of auxin flow, and the width of the arrow is proportionate to the capacity of a cell to transport auxin. **A** Most cells have a similar capacity to transport auxin. **B** Increased auxin flow in some cells leads to an increase in their capacity to transport auxin. **C** Specialisation of cells to transport auxin drains auxin from the surrounding tissues and leads to vascular bundle formation. Modified from Turner and Sieburth (2003).

Initially, parenchymatic cells, which are all competent for transdifferentiation into vessels, compete for a limited supply of auxin. Some of these cells will transport more auxin than their neighbours and thus deplete them from auxin causing a draining effect. The differentiation is accelerated depending on the flux of auxin that has passed through the cell. Conversely, the capacity for polar auxin flux grows with progressive differentiation.

This self-amplifying, positive feedback loop in combination with lateral inhibition caused by mutual competition for auxin will result in an ordered pattern of vascular tissue. The auxin-canalisation model has been extensively studied and mathematically modelled. For instance, it is capable to predict venation patterns in leaves (for review, see Berleth and Sachs, 2001).

The auxin-canalisation model places the directionality of auxin transport into the center of plant patterning. Therefore, the identification of the cellular and molecular mechanisms responsible for this directionality has become a central topic in plant developmental biology.

1.4 Polar auxin transport is mediated by polarly localised efflux carriers

The principal naturally occurring auxin (indole-3-acetic acid, IAA), an indolic compound related to the amino acid tryptophan, is synthesised in meristematic regions of the shoot apex and is transported basipetally to the root tip. This polarised auxin flow provides essential directional and positional information for developmental processes, such as embryogenesis, apical dominance, organ formation and tropistic growth.

Remarkably, the existence of a polar transport mechanism was already described by the Darwins, who postulated the involvement of a “transmissible signal” in the regulation of plant organ growth (Darwin and Darwin, 1881). In 1926, Went demonstrated that an externally applied regulator can induce the bending of plants, and the responsible substance was later named auxin. In the 1930s, Cholodny and Went hypothesised that differential transport of auxin in plants results in asymmetric cell elongation, thereby giving rise to tropistic growth responses to environmental stimuli (Cholodny, 1928; Went and Thimann, 1937). However, the mechanisms underlying auxin distribution in plants have remained largely unknown.

It took another 40 years until the establishment of a directional flow could be derived from cellular aspects of auxin transport. The polar transport of auxin is a cell-to-cell process that has been described in a nowadays widely accepted chemiosmotic model for auxin transport (Rubery and Sheldrake, 1974; Raven, 1975; for review, see Lomax et al., 1995) (**Fig. 3**).

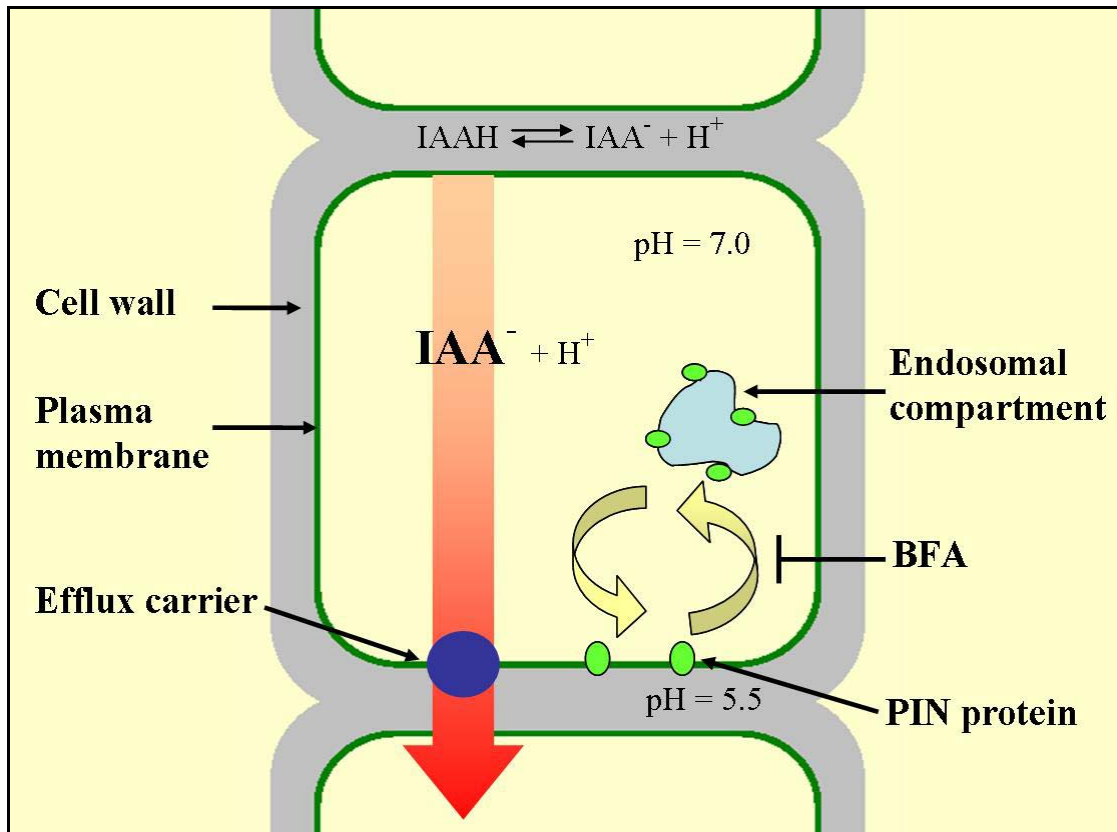


Figure 3: Chemiosmotic model for polar auxin transport. In the acidic apoplast, IAA is mostly present in the protonated form (IAAH) and can enter the cell mainly by diffusion. Due to a higher pH inside the cell, IAA is deprotonated (IAA⁻) and thereby trapped in the cell. Active efflux by auxin efflux carriers is required for further transport of auxin. Asymmetric distribution of the efflux carrier at the plasma membrane ensures directional transport. *Pin-formed* (PIN) proteins cycle between the plasma membrane and endosomal compartments. This constitutive cycling can be blocked by the inhibitor Brefeldin A (BFA).

The model is based on the observation that only the protonated form of auxin (IAAH) can pass the plasma membrane, whereas the auxin anion (IAA⁻) is unable to cross the membrane. Extracellular apoplastic auxin, which is predominantly protonated, first enters the cell mainly through passive diffusion. Once inside the cell, the higher intracellular pH causes the protonated form of auxin to deprotonate resulting in the symplastic accumulation of auxin anions. Efflux of the trapped auxin anions is then only possible, if mediated by efflux carrier proteins that transport IAA⁻ through the plasma membrane back into the surrounding apoplast. Therefore, the polarity of auxin transport results from an asymmetric distribution of efflux carriers.

In the meantime, some of the molecular mechanisms and the responsible molecular players involved in the polar transport of auxin have been identified.

1.5 Components of the auxin-transport machinery

1.5.1 *Pin-formed* proteins

The chemiosmotic hypothesis explains the directionality of auxin transport by a polar subcellular localisation of auxin-efflux carriers.

In the meantime, several plant-specific *pin-formed* (PIN) plasma-membrane proteins have been identified as important candidates for auxin-efflux facilitator proteins (for review, see Chen and Masson, 2006).

A mutation in the *Pin1* gene was first identified by Okada and colleagues, who reported the isolation of a mutant producing inflorescence axes that almost entirely lacked flowers (Okada et al., 1991). This mutant was named *pin-formed* or *pin1* due to the needle-like phenotype of the inflorescences and gave its name to the entire protein family. The PIN proteins contain six to ten transmembrane domains and exhibit weak similarities to bacterial transporters (Gälweiler et al., 1998).

Their abundance differs between the two poles of a given cell. This gradient correlates with the direction of auxin flow in different parts of the plant (for review, see Friml, 2003). Thus, the localisation of PIN proteins represents a valuable molecular marker for cell polarity.

Consistent with the presumed function of PIN proteins in auxin transport, the phenotype of the *pin1* mutant can be mimicked by inhibitors of polar auxin transport. The most widely used inhibitors of auxin efflux are 1-*N*-naphthylphthalamic acid (NPA) and 2,3,5-triiodobenzoic acid (TIBA) which belong to a group of inhibitors known as phytotropins (Rubery, 1990). The

application of these inhibitors to plant tissues results typically in an increase in auxin accumulation, presumably caused by the inhibition of auxin efflux activity (Morris et al., 2004).

1.5.2 Targeted vesicle flow ensures the polar localisation of auxin-efflux carriers

Signalling molecules can regulate cellular behaviour by modulating the subcellular distribution of proteins. One important mechanism in this mode of regulation is a specific, directed vesicle traffic, termed constitutive cycling, which consists of repeated internalisation and recycling of proteins to and from the plasma membrane.

PIN proteins are a good example for this constitutive recycling between plasma membranes and intracellular endosomal compartments (Geldner et al., 2001; Paciorek et al., 2005) (**Fig. 3**, p. 8). The physiological relevance of such cycling might be to tightly control the number of efflux-carrier molecules, thus ensuring fine-tuning of auxin efflux. This recycling seems to be under control of small GTPases, the ADP-ribosylation factors (ARFs) and their associated guanine nucleotide exchange factors (Geldner et al., 2003). A mutation of one of these guanine nucleotide exchange factors (ARF-GEFs) is responsible for the above-mentioned *gnom* phenotype and results in mislocalisation of PIN1 that becomes trapped in intracellular compartments. This cellular phenotype of the mutant can be phenocopied by treatment of the wild type with Brefeldin A (BFA), a fungal toxin that selectively blocks ARF-GEFs (Geldner et al., 2001). This suggests that ARF-dependent vesicle trafficking is involved in the polar distribution of PIN proteins and thus in cell polarity.

Interestingly, the modulation of PIN protein trafficking was shown to be regulated by auxin itself (Paciorek et al., 2005), providing a mechanism for the self-amplifying feedback regulation of auxin transport on the molecular level.

1.5.3 Actin assists the polar targeting of the auxin-efflux complex

The reversible effect of BFA on PIN1 internalisation and cycling is interrupted in the presence of Cytochalasin D, a drug that eliminates actin filaments. This indicates that the endosomal exocytosis of PIN1 is actin-dependent (Geldner et al., 2001). In contrast to animal cells, the dynamics of endoplasmatic reticulum and Golgi apparatus are not controlled by microtubules and their associated motors, dyneins and kinesins, but are fully under control of actomyosin. This leads to the conclusion that the direction of targeted vesicle traffic in the context of polar auxin transport might be defined by a specified orientation of the actin cytoskeleton.

In addition, several lines of evidence indicate that ARF-dependent vesicle trafficking and polar auxin transport are related to actin filaments:

1. The idea that the signalling role of auxin is related to intracellular traffic is actually quite old, because interruption of the actin cytoskeleton stops cytoplasmic streaming, a key phenomenon of living plant cells. Already during the classical period of auxin research, Sweeney and Thimann (1937) proposed that auxin might induce coleoptile growth by stimulating cytoplasmic streaming. In the 1990s, Thimann returned to this idea and was able to show that auxin-dependent growth could be very efficiently blocked by the elimination of actin (Thimann et al., 1992).
2. When auxin transport was inhibited by phytotropins in zygotes of the brown alga *Fucus*, both the organisation of actin filaments and the induction of developmental polarity by light or gravity were impaired (Sun et al., 2004). Conversely, the application of actin-eliminating drugs resulted in reduced polar auxin transport in maize coleoptiles (Cande et al., 1973) and in zucchini hypocotyls (Butler et al., 1998).

3. A link between actin and auxin signalling has also been proposed from studies on auxin-dependent cell growth in Graminean coleoptiles. In this model, the auxin-dependent reorganisation of actin filaments into fine cortical strands could be shown to correlate with the auxin response of growth (Waller et al., 2002). Upon treatment with BFA, actin became trapped on the endomembrane system and was partitioned into the microsomal fraction. The cellular correlate of this trapping was a bundling of cortical actin strands into dense bundles. It was accompanied by a shift of the dose-response of auxin-dependent cell elongation towards higher concentrations. Thus, a bundling of actin resulted in a reduced sensitivity of cell growth to auxin. These observations linked auxin signalling, vesicle flow, and the organisation of actin filaments, suggesting that microfilaments might transport vesicles. However, the causal relationship between these three events remained unresolved.

4. The actin cytoskeleton has also been implicated in the regulation of gravitropism, because interruption of intact actin filaments by the actin inhibitor Latrunculin B (LatB) promoted the gravitropic responses in different plant species (Hou et al., 2004) producing an enhanced curvature response of the roots. The effect of LatB impaired the fine meshwork of actin filaments in different regions of the treated roots, altered the dynamics of amyloplast sedimentation in the columella cells, and prolonged the intracellular alkalinisation response. These abnormalities were accompanied by a persistent auxin gradient in the root cap.

1.5.4 The ARP2/3 complex nucleates actin polymerisation in a polarly and spatially controlled manner

Actin organisation is controlled by several, partially directly actin-associated protein complexes including the Rho-related GTPases of plants (ROPs), the WAVE (for Wiskott-Aldrich syndrome protein family verproline homologous) complex and the actin-related protein (ARP) 2/3 complex. These regulators modulate the actin cytoskeleton through an elaborate signalling network (for review, see Xu and Scheres, 2005). Interestingly, the function of ROPs is dependent on ARFs, i.e. the key players for the polar localisation of PIN proteins. Since the ROP proteins interact directly with upstream regulators of the ARP2/3 complex, they might link the auxin-signalling machinery to actin organisation.

The ARP2/3 complex is a modulator of the actin cytoskeleton conserved through eukaryotic evolution (Vartiainen and Machesky, 2004). It is essential for amoeboid locomotion and subcellular motility of organelles. When activated, it enhances the nucleation and polymerisation of filamentous actin, such that the ARP2/3 complex caps the pointed end, and the actin filament grows in direction of the barbed end (Mullins et al., 1998; Svitkina and Borisy, 1999; Blanchoin et al., 2000). Upon binding to existing actin filaments, the ARP2/3 complex can initiate branches and generate dynamic actin arrays. ARP2 and ARP3 are the largest of seven subunits composing the multiprotein ARP2/3 complex and share significant structural and sequence similarity with actin (Robinson et al., 2001). In animal cells, this complex has been shown to participate in protrusion-mediated motility. Although plant cells are not endowed with motility, the ARP2/3 complex was found to be essential for developmental changes of cell polarity and shape (for review, see Mathur, 2005).

Homologues of all seven subunits of the ARP2/3 complex have recently been identified in plants on the basis of homology searches and loss-of-function mutants. Mutations in genes that encode subunits of the ARP2/3 complex lead

to increased bundling of filamentous actin and the formation of aberrant actin patches, culminating in misdirected expansion of various cell types including trichomes, pavement cells, hypocotyl cells and root-hair cells (Mathur et al., 2003; Li et al., 2003; Le et al., 2003; El-Assal et al., 2004; Saedler et al., 2004). The randomly misshapen trichomes of this mutant class (classified as *distorted* mutants) could be phenocopied in wild-type leaves by pharmacological manipulation of actin (Mathur et al., 1999; Szymanski et al., 1999). Thus, these mutant phenotypes reveal an important role for actin microfilaments and the ARP2/3 complex in the control of polar cell expansion. In cells with pronounced tip growth, such as rhizoids of germinated fucoid zygotes (Hable and Kropf, 2005) or extending root hairs (Van Gestel et al., 2003), elements of this complex could be immunolocalised to the leading edge of these cells, i.e. to the site where actin filaments elongate. Independent observations on apical extension and actin dynamics in tip-growing pollen tubes speak for a major role of actin polymerisation in polarised cell expansion (Vidali et al., 2001; Vidali and Hepler, 2001). Since ARP2 and ARP3 were found to localise to sites of actin-filament nucleation in tobacco BY-2 cells (Fišerová et al., 2006), the two proteins can be used as markers for the polarity of actin filaments in plants. However, in plants, the components of the ARP2/3 complex have not been visualised *in vivo* so far.

1.6 Scope of the dissertation

A mounting body of evidence suggests that actin microfilaments and the polar transport of the plant hormone auxin play central roles in the induction and maintenance of plant-cell polarity, which in turn is the mainspring for pattern formation.

The present work is focussing on the link between actin polarity and auxin-regulated patterns of cell division. Cell division is a key event for patterning, because it lays down the spatial constraints of subsequent cell growth. Whereas

one cell pole can be inherited from the mother cell, there must be a *de-novo* generation of a new cell pole at the site, where a new cross wall is laid down. Which role play the microfilaments that are elements of auxin-triggered regulatory circuits during patterned cell division?

In general, an intact actin cytoskeleton is required for functional auxin responses leading to ordered pattern formation. Vesicles containing components of auxin signalling might be transported along actin in a certain direction. Since the organisation of actin in turn depends on auxin, this constitutes a self-amplification loop between auxin signalling and actin filaments.

The scope of the present work is to directly demonstrate the causal relationship between auxin signalling, vesicle flow, and the organisation of actin filaments within this loop. Thus, it is necessary to dissect and manipulate individual elements in this non-linear, self-referring system. If actin is part of an auxin-driven feedback loop, it should be possible to manipulate auxin-dependent patterning through manipulation of actin. In particular, this work is investigating whether the bundling of actin will impair the polarity of auxin flow. For this purpose, patterned cell division is used as sensitive trait to monitor changes of polar auxin fluxes.

Moreover, if the arrangement of actin filaments is important for pattern formation, then the polarity of actin filaments would decide over patterning via the transport of components necessary for auxin signalling. This reasoning leads to the question, whether the polarity of individual actin filaments is related to the polarity of the entire cell. Thus, it is necessary to visualise microfilament polarity in the context of cell polarity using both markers for actin nucleation (ARP) and polar auxin transport (PIN).

1.7 The tobacco cell line BY-2 as a model system for auxin-dependent, supracellular patterning of cell divisions

The use of the model *Nicotiana tabacum* L. cv. Bright Yellow 2 (BY-2) has generated a wealth of data on the role of phytohormones during the plant cell cycle (Nagata et al., 1992). The possibility to synchronise BY-2 cells (Nagata and Kumagai, 1999) provided a powerful approach to detect fluctuations of hormone levels during cell division (Redig et al., 1996).

In contrast to other tobacco cell lines, the BY-2 cell line is widely utilised in plant cell biology and a panel of numerous fluorescent marker lines is available. BY-2 cell cultures can be maintained with a simple medium (modified Murashige and Skoog medium; Murashige and Skoog, 1962). Since BY-2 cells grow rapidly during a seven-day period and do not aggregate, a large number of uniform and relatively large cells can be analysed. The BY-2 cells contain small non-photosynthetic plastids, such that fluorescence microscopy is not affected by chlorophyll autofluorescence. Last but not least, BY-2 cells can be easily transformed in a manageable period both by biolistic or *Agrobacterium*-mediated transformation.

In the present work, the tobacco cell line BY-2 is utilised as a model system to study intracellular communication in patterning with focus on supracellular patterning and the roles of auxin and actin therein. The BY-2 cell line is characterised by well defined axial cell divisions that generate pluricellular, polar cell files exhibiting basic features of pattern formation (**Fig. 4**). This aspect of the BY-2 cell line has not been exploited so far, but allows to investigate patterning in a field, where the number of elements increases during the patterning process reflecting the general situation in plants. Furthermore, the directional flow of auxin within cell files can be inhibited in this cell line by 1-*N*-naphthylphthalamic acid (NPA) and other phytochemicals at conditions that do not

affect the structure of the cytoskeleton (Petrášek et al., 2003). Therefore, this system is well suited to study spatial aspects of patterned cell division.

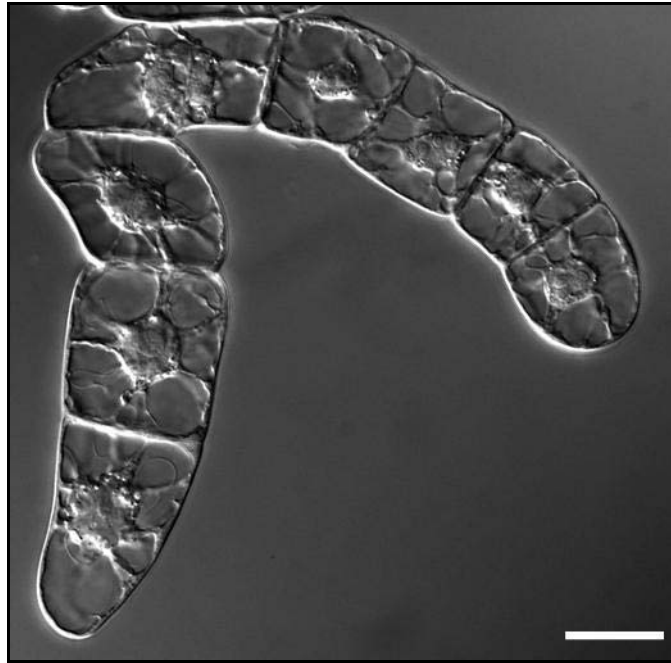


Figure 4: The tobacco cell line BY-2 (*Nicotiana tabacum* L. cv. Bright Yellow 2). This cell line grows in simple files that exhibit basic characteristics of pattern formation, such as a clear axis and polarity of cell division and growth. Bar = 20 μm .

2. Materials and Methods

2.1 Tobacco cell cultures

The tobacco cell line BY-2 (*Nicotiana tabacum* L. cv. Bright Yellow 2; Nagata et al., 1992) was cultivated in liquid medium containing 4.3 g/L Murashige and Skoog salts (Duchefa, Haarlem, the Netherlands), 30 g/L sucrose, 200 mg/L KH_2PO_4 , 100 mg/L inositol, 1 mg/L thiamine and 0.2 mg/L* 2,4-dichlorophenoxyacetic acid (2,4-D), pH 5.8. Cells were subcultured weekly, inoculating 1.5-2 mL of stationary cells into 30 mL of fresh medium in 100-mL Erlenmeyer flasks. The cell suspensions were incubated at 25°C in the dark on an orbital shaker (KS250 basic, IKA Labor Technik, Staufen, Germany) at 150 rpm. Stock BY-2 calli were maintained on media solidified with 0.8% (w/v) agar and subcultured monthly. Transgenic cells and calli were maintained on the same media supplemented with either 30 mg/L hygromycin (BY-2 YFP-mT cell line) or 25 mg/L kanamycin (BY-2 GFP-FABD2 cell line and BY-2 GFP-PIN1 cell line). In some experiments, the cell lines were assessed in the absence of selective pressure, but without any differences in patterning or arrangement of actin filaments.

The BY-2 GFP-PIN1 cell line was kindly provided by Dr. J. Petrášek (Institute of Experimental Botany, Academy of Sciences of the Czech Republic, Prague, Czech Republic), who stably transformed BY-2 cells with a fusion construct between PIN1 (from *Arabidopsis thaliana*) and GFP (Benková et al., 2003).

* 0.2 mg/L 2,4-D is equivalent to 0.9 μM 2,4-D.

2.2 Constructs

2.2.1 *pVKH18En6-YFP-talin* construct

The *p35S-YFP-talin* construct (Brandizzi et al., 2002) within a binary vector (*pVKH18En6*) was a kind gift of Dr. F. Brandizzi (Research School of Biological and Molecular Sciences, Oxford Brookes University, UK).

2.2.2 *pK7WGF2-FABD2* construct

The region encoding the second fimbrin actin-binding domain (FABD2; amino acids 325-687) of the *Arabidopsis thaliana* fimbrin 1 protein (AtFim1) was amplified by PCR from *pGFPm3abd2* (Voigt et al., 2005; for details, see **Appendix**, p. 83) using the following primers: 5'-GGGG ACA AGT TTG TAC AAA AAA GCA GGC TTG GAT CCT CTT G-3' and 5'-GGGG AC CAC TTT GTA CAA GAA AGC TGG GTT CTA TTC GAT GGA TGC TTC CT-3'. The underlined sites represent the *att* sites that have to be integrated into the PCR product for the Gateway[®] recombination reactions (Hartley et al., 2000).

For the generation of stably transformed tobacco cells, the resulting *Fabd2* region was inserted into the binary vector *pK7WGF2* (Karimi et al., 2002; Karimi et al., 2005; for details, see **Appendix**, p. 88) employing the Gateway[®] technology (Invitrogen Corporation, Paisley, UK) according to the manufacturer's protocol (for details, see **Appendix**, pp. 85ff). The plasmid was sequenced to confirm the accuracy of the sequence. The obtained construct, *pK7WGF2-FABD2*, was a C-terminal fusion of the second fimbrin actin-binding domain to GFP.

2.2.3 p2GWR7-ARP3 construct

For transient expression of the actin-related protein 3 (ARP3) in tobacco BY-2 cells, the coding sequence of *Nicotiana tabacum Arp3* (for details, see **Appendix**, p. 84) was amplified by PCR from *psmGFP-ARP3*, kindly provided by Dr. J. Fišerová, (Department of Botany, Faculty of Science, Charles University Prague, Czech Republic), using the following primers: 5'-GGGG ACA AGT TTG TAC AAA AAA GCA GGC TAT ATG GAC CCT TCT ACC TCT CG-3' and 5'-GGGG AC CAC TTT GTA CAA GAA AGC TGG GTT TCA ATA CAT TCC CTT GAA TAC AGG-3'. The *Arp3* region was then inserted into the transient expression vector p2GWR7 (Dr. R. Y. Tsien, University of California, San Diego, USA; Campell et al., 2002; for details, see **Appendix**, p. 89) as described above resulting in *p2GWR7-ARP3*, an N-terminal fusion of the actin-related protein 3 to RFP. The plasmid was sequenced to confirm the accuracy of the sequence.

2.3 *In silico* analysis

The confirmed sequence of the putative tobacco *Arp3* (*NtArp3*) was used for a similarity search on the amino-acid level in the Swiss-Prot data base (<http://www.expasy.org>; for Swiss-Prot accession numbers, see **Appendix**, p. 90) using a BlastP routine with standard settings. The best hits (E-value e^{-122} or smaller) of this search were ARP3 homologues from other organisms. These sequences were aligned using the KALIGN software (<http://msa.cgb.ki.se/cgi-bin/msa.cgi>; Lassmann and Sonnhammer, 2005) with standard settings. This alignment was imported in FASTA-format into the ClustalW software (<http://www.ebi.ac.uk/clustalw/index.html>) and used to produce a cladogram based on the neighbour-joining method (Saitou and Nei, 1987) that could be viewed using the TreeView software (<http://taxonomy.zoology.gla.ac.uk>). The

domains in the sequence were defined using the ProDom database (<http://prodom.prabi.fr>).

2.4 Transformation and establishment of tobacco BY-2 cells

2.4.1 Biolistic, stable expression of YFP-mT

For biolistic transformation, gold particles (1.5–3.0 μm ; Sigma-Aldrich, Steinheim, Germany) were coated with the *p35S-YFP-talin* vector construct according to a slightly modified manual of BIO-RAD (PDS-1000/He Particle Delivery System Manual; for details, see **Appendix**, p. 91). An amount of 1 μg DNA was used for transfection. DNA-coated gold particles were placed on macrocarriers (BIO-RAD, Hercules, CA, USA). A cell suspension of 3-day-old BY-2 cells was filtrated onto filter paper. Filtrated BY-2 cells were placed in a particle gun that was constructed according to Finer et al. (1992) and bombarded by three shots at a pressure of 1.5 bar in the vacuum chamber at -0.8 bar. Following bombardment, which was performed under sterile conditions, cells were diluted into liquid medium and kept in the dark at 25°C. After incubation for 24 h, the cells were plated onto solid medium containing 30 mg/L hygromycin. Hygromycin-resistant calli, which appeared after 28 days, were transferred onto new plates and cultured independently until they reached approximately 1 cm in diameter. Cell-suspension cultures established from these calli were maintained as described above, with addition of 30 mg/L hygromycin to the cultivation medium. After six weeks a YFP-mT cell line suitable for observing actin filaments was selected by examination of YFP-fluorescence by fluorescence microscopy.

2.4.2 Biolistic, transient expression of RFP-ARP3

For biolistic transformation, gold particles (1.5–3.0 μm ; Sigma-Aldrich) were coated with the RFP-ARP3 vector construct (*p2GWR7-ARP3*) as described above.

A cell suspension of 3-day-old transgenic BY-2 GFP-FABD2 cells was transferred into PetriSlides™ (Millipore, Billerica, USA) containing solid medium. The transgenic BY-2 cells were placed in a particle gun that was constructed according to Finer et al. (1992) and bombarded by three shots at a pressure of 1.5 bar in the vacuum chamber at -0.8 bar. Following bombardment, cells were kept in the dark at 25°C for 18-60 h before observation.

2.4.3 *Agrobacterium*-mediated, stable expression of GFP-FABD2

The binary vector construct *pK7WGF2-FABD2* was introduced into *Agrobacterium tumefaciens* (strain LBA4404) by heat shock. A 4-mL aliquot of BY-2 cells that had been cultivated for 3 days was co-incubated for further 3 days with 100 μL of an overnight culture of the transformed *Agrobacterium tumefaciens* at 27°C as described by An (1985). After incubation, the cells were washed three times in liquid medium containing 100 mg/L cefotaxim and were then plated onto solid medium containing 100 mg/L kanamycin and 100 mg/L cefotaxim. Kanamycin-resistant calli, which appeared after 28 days of incubation in the dark at 25°C, were transferred onto new plates and cultured separately until they reached approximately 1 cm in diameter. Cell-suspension cultures established from these calli were maintained as described above, with addition of 25 mg/L kanamycin to the cultivation medium. After six weeks, a cell line suitable for observing microfilaments was selected by examination of GFP-fluorescence by fluorescence microscopy to yield the cell line BY-2 GFP-FABD2.

2.5 Phytotropin and auxin treatments

1-*N*-naphthylphthalamic acid (NPA) was synthesised by Dr. W. Michalke (Institute for Biology III, University of Freiburg, Germany) according to Thompson et al. (1973). NPA and 2,3,5-triiodobenzoic acid (TIBA; Duchefa) were added at inoculation from filter-sterilised stocks of 10 mM in dimethyl sulphoxide to final concentrations of 3, 12 or 30 μ M. Auxins were also directly added to the final concentration of 2 μ M into the standard culture medium using filter-sterilised stocks of 10 mg/mL indole-3-acetic acid (IAA; Sigma-Aldrich), 10 mg/mL 1-naphthaleneacetic acid (NAA; Roth, Karlsruhe, Germany) and 10 mg/mL 2,4-dichlorophenoxyacetic acid (2,4-D; Sigma-Aldrich) dissolved in 96% (v/v) ethanol, respectively. Equal aliquots of sterile dimethyl sulphoxide and ethanol were added to the control samples.

2.6 Latrunculin B treatment, cold treatment, and recovery experiments

Following particle bombardment with the RFP-ARP3 construct, BY-2 GFP-FABD2 cells were diluted in liquid medium containing 500 nM Latrunculin B (LatB; Sigma-Aldrich) that was added from a stock solution of 2.5 mM LatB in 96% (v/v) ethanol. To eliminate actin filaments for subsequent recovery experiments, the cell suspension was kept in the dark for 10 h at 25°C. Thereafter, the cells were washed four times in fresh medium to remove LatB and observed immediately.

For the cold treatment, the cells were stored in a refrigerator at 2°C for 10 h after transient transformation. Subsequently, they were resuspended in liquid medium at the control temperature of 25°C and observed immediately.

2.7 Visualisation of actin filaments by rhodamine-phalloidin staining

Actin filaments were visualised by the method of Kakimoto and Shibaoka (1987) modified according to Olyslaegers and Verbelen (1998). Suspended BY-2 cells were fixed for 10 min in 1.8% (w/v) paraformaldehyde (PFA) in standard buffer (0.1 M 1,4-piperazin-diethane sulfonic acid - PIPES [pH 7.0], supplemented with 5 mM MgCl₂, and 10 mM ethylene glycol bis(2-aminoethyl) tetraacetic acid - EGTA). After a subsequent 10-min fixation in standard buffer containing 1% (v/v) glycerol, cells were rinsed twice for 10 min with standard buffer. Then, 0.5 mL of the resuspended cells were incubated for 35 min with 0.5 mL of 0.66 μM TRITC-phalloidin (Sigma-Aldrich) prepared freshly from a 6.6 μM stock solution in 96% (v/v) ethanol by dilution (1:10 [v/v]) with phosphate buffered saline (PBS; 0.15 M NaCl, 2.7 mM KCl, 1.2 mM KH₂PO₄, and 6.5 mM Na₂HPO₄ [pH 7.2]). Cells were then washed three times for 10 min in PBS and observed immediately.

The same protocol was used for the co-localisation experiments of YFP-mT or GFP-FABD2 and rhodamine-phalloidin in BY-2 cells overexpressing YFP-mT or GFP-FABD2, respectively.

2.8 Quantification of pattern and morphology

2.8.1 Determination of frequency distributions and cell elongation

From each sample, 0.5-mL aliquots of cells were collected four days after inoculation and immediately viewed under an AxioImager Z.1 microscope (Zeiss, Jena, Germany). Differential interference contrast (DIC) images were

obtained by a digital imaging system (AxioVision, Rel. 4.5; Zeiss, Jena, Germany) and frequency distributions over the number of cells per individual file were constructed. Cell length and width were also determined from the central section of the cells using the length function of the AxioVision software. Cell elongation was calculated as ratio of cell length over cell width. Each data point represents 3000 cell files or cells from three independent experimental series. The results were tested for significance by a Student's t-test at the 95% confidence level.

2.8.2 Determination of cell viability and cell density

Cell viability was analysed by the Trypan Blue dye exclusion test (Phillips, 1973). Aliquots (0.5 mL) from each sample were stained with 0.4% (w/v) Trypan Blue solution (Sigma-Aldrich) at a ratio of 1:100 (v/v). After incubation for 3 min, the frequency of the unstained (viable) cells was determined as well as the cell number per mL using a Fuchs-Rosenthal hemacytometer under bright-field illumination. For each individual sample, 1000 cells were scored.

2.8.3 Determination of mitotic indices

For the mitotic indices, 0.5-mL aliquots of cell suspension were fixed in Carnoy fixative (3:1 [v/v] 96% [v/v] ethanol:glacial acetic acid) plus 0.25% Triton X-100 and stained with 2'-(4-Hydroxyphenyl)-5-(4-methyl-1-piperazinyl)-2,5'-bi(1H-benzimidazole)-trihydrochloride (Hoechst 33258, Sigma-Aldrich), which was prepared as a 0.5 mg/mL filter-sterilised stock solution in distilled water and used at a final concentration of 1 µg/mL. Cells were recorded under an AxioImager Z.1 microscope (Zeiss) using the filter set 49 DAPI (excitation at 365 nm, beamsplitter at 395 nm and emission at 445 nm). The mitotic indices were calculated as the number of cells in mitosis divided by the total number of cells counted. For each time point, 1000 cells were scored.

2.8.4 Quantification of ARP3-expression patterns

For the quantification of the ARP3 distribution within cell files, projections of serial sections of transiently transformed tobacco cells were constructed using the maximum projection function of the AxioVision software (Zeiss). The cells were categorised into two classes (terminal cells of a file or cells of the central region of the file). Each cell was divided into two halves, and the number of ARP3 dots over the cross-sectional area in the central plane of the cell (subtracted by the cross-sectional area occupied by the nucleus) was determined using the outline function of the AxioVision software.

For each value, 50 terminal cells and 50 central cells were used. The results were tested for significance by a Student's t-test at the 95% confidence level.

2.9 Microscopy and image analysis

BY-2 cells were examined under an AxioImager Z.1 microscope (Zeiss) equipped with an ApoTome microscope slider for optical sectioning and a cooled digital CCD camera (AxioCam MRm).

TRITC and RFP fluorescence were observed through the filter set 43 HE (excitation at 550 nm, beamsplitter at 570 nm and emission at 605 nm). YFP and GFP fluorescence were recorded through the filter sets 46 HE (excitation at 500 nm, beamsplitter at 515 nm and emission at 535 nm) and 38 HE (excitation at 470 nm, beamsplitter at 495 nm and emission at 525 nm), respectively, using either a 63x plan apochromat oil-immersion objective or a 40x objective. Stacks of optical sections were acquired at different step sizes between 0.5 and 0.8 μm .

For analysis of division pattern, cells were observed under the same microscope with a 20x objective and differential interference contrast (DIC) illumination.

Images were processed and analysed using the AxioVision software (Zeiss) as described above. For publication, images were processed with respect to contrast and brightness using the Photoshop software (Adobe Systems, San Jose, CA, USA).

3. Results

3.1 The impact of actin organisation on patterned cell division in BY-2 cell files

Since actin seems to play a role for polar auxin transport, I induced a specific change in actin organisation (hypertrophic bundling) and studied the effect of this changed actin organisation on a physiological process that depends on polar auxin transport. Previous work (Campanoni et al., 2003) had shown that cell division was synchronised by polar auxin transport in the tobacco cell line VBI-0 (*Nicotiana tabacum* L. cv. Virginia Bright Italia 0). Since VBI-0 is recalcitrant to transformation, it was necessary to change to the widely used tobacco cell line BY-2. Hence, it was essential to check, whether this cell line, similar to VBI-0, exhibited patterns of cell division that are under control of polar auxin transport (3.1.1). In the next step, I induced constitutive bundling of actin by overexpression of the actin-binding protein mouse-talin (3.1.2). This constitutive bundling interferes with polar patterning (3.1.3). Typical patterning, indicating a rescue of polar auxin transport, could be restored by recovery of a normal (unbundled) actin organisation in response to exogenous transportable auxins (3.1.4).

3.1.1 Cell division within cell files of BY-2 is synchronised by a NPA-sensitive signal

In order to assess cell division patterns, the onset of the stationary phase had to be defined by following the time course of cell division in non-transformed BY-2 cells and in BY-2 cells overexpressing YFP-mouse talin (YFP-mT). Although cell division activity in the YFP-mT line was delayed by about 0.5-1 days and

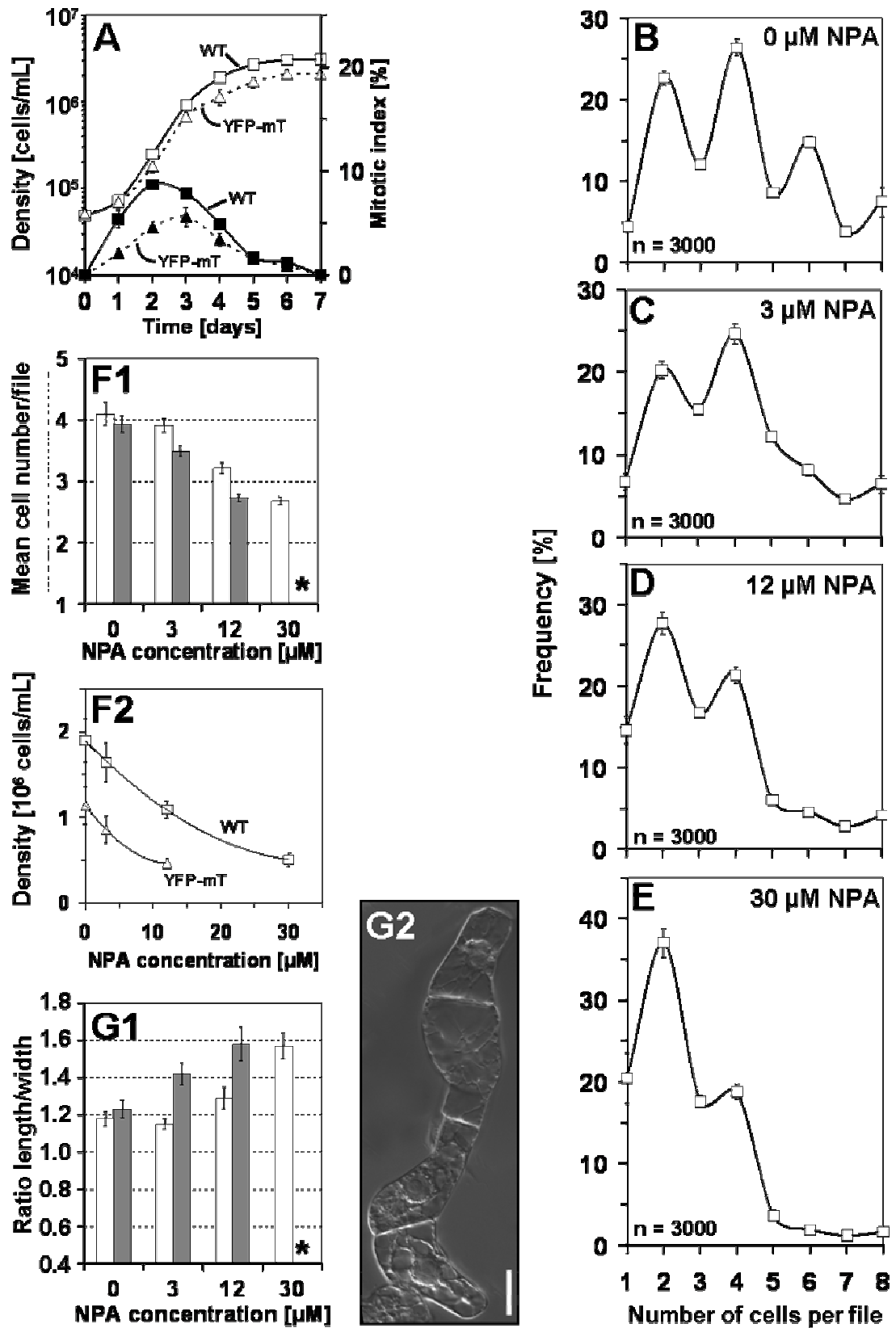
reduced in amplitude, the temporal pattern was very similar and cell density approached a plateau from 4 days after subcultivation (**Fig. 5A**). Thus, frequency distributions over the cell number per individual file were constructed at this point of time.

Under standard cultivation conditions, the frequency distribution of non-transformed BY-2 cells exhibited characteristic peaks of frequency for files composed of two, four and six cells (**Fig. 5B**). Similar distributions were observed throughout the entire exponential phase (data not shown). Thus, files with even cell numbers are more frequent than files with uneven cell numbers.

In the next step, I asked whether this characteristic pattern was related to auxin transport. Therefore, BY-2 cells were inoculated in presence of 3 or 12 μM 1-*N*-naphthylphthalamic acid (NPA), an inhibitor of polar auxin transport. The concentrations were chosen such that neither polarity and axially of cell files nor their viability (for details, see **Appendix**, p. 92) were affected. What was affected under these conditions was the distribution of cell division (**Fig. 5, C and D**). Treatment with these low concentrations of NPA progressively equalised the frequencies of files with even and uneven cell numbers - especially for files with a higher number of cells. It should be noted that, at 3 μM NPA, cell division (**Fig. 5, F1 and F2**) was only slightly reduced, and cell elongation (**Fig. 5G1**) was not affected at all. From 12 μM NPA the inhibition of cell division became evident (**Fig. 5, F1 and F2**), and cell elongation increased progressively (**Fig. 5G1**). However, for a high (30 μM) concentration of NPA, the upper two frequency peaks disappeared (**Fig. 5E**), and files with more than four cells became very rare. Under these conditions, I observed a strong inhibition of cell division (**Fig. 5, F1 and F2**) and a significant stimulation of cell elongation (**Fig. 5G1**) that were accompanied by a loss of file polarity and axially. Although the cells significantly increased in length, they exhibited localised swellings resulting in irregular, bulbous cell shapes (**Fig. 5G2**). In addition, the difference between the more pointed terminal cells of a file and the more isodiametric cells in the centre of a file vanished progressively.

► **Figure 5:** Cell division in non-transformed BY-2 cells follows a pattern that depends on polar auxin fluxes. **A** Cell density (*open symbols*) and mitotic indices (*closed symbols*) over time after subcultivation of non-transformed BY-2 cells (WT, *squares, solid curves*) and BY-2 cells overexpressing YFP-mouse talin (YFP-mT, *triangles, dotted curves*). Each point represents the mean from 1000 scored cells. **B-E** Frequency distribution over cell number per file in non-transformed BY-2 cells at day 4 after inoculation in the absence of NPA (**B**) or in presence of 3 (**C**), 12 (**D**) or 30 (**E**) μM NPA. Error bars indicate SE. **F, G** Effect of NPA on cell division (**F1, F2**) and cell elongation (**G1**) in non-transformed BY-2 cells (*white bars*) versus cells overexpressing YFP-talin (YFP-mT, *grey bars*) at day 4 after inoculation. Each distribution is based on 3000 individual cells from three independent experimental series. Cell division is plotted as mean number of cells per file (**F1**) and as cell density (**F2**), cell elongation as ratio of cell length over cell width (**G1**). Error bars indicate SE. *Asterisks:* YFP-mT cells died at 30 μM NPA, such that a measurement of length-width ratio was not meaningful. **G2** Morphology of non-transformed BY-2 cells after treatment with 30 μM NPA. Bar = 20 μm .

Figure 5



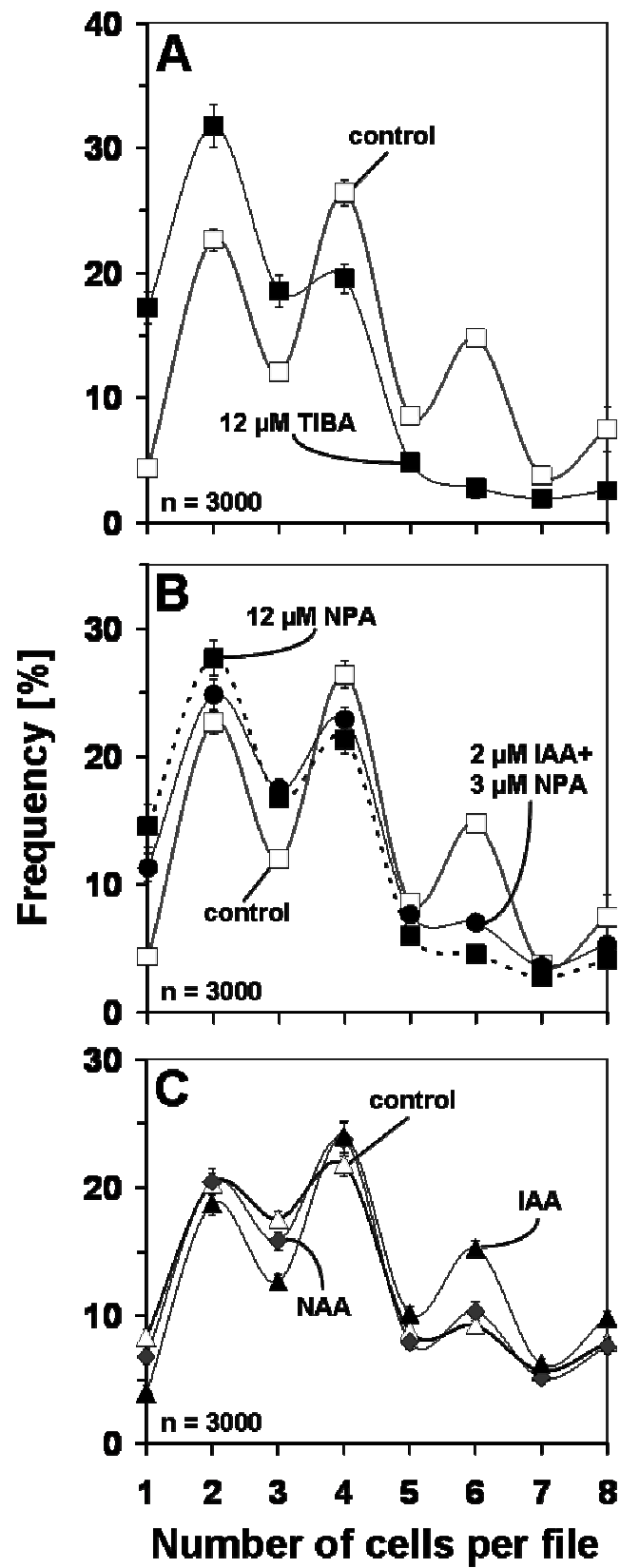
In order to test whether the loss of synchrony was limited to NPA or whether it could be induced by other inhibitors of polar auxin flow, I analysed the effect of 12 μM 2,3,5-triodobenzoic acid (TIBA) and observed that, similar to NPA, the synchrony of cell division was lost such that the difference in the frequency between even and uneven cell numbers disappeared (**Fig. 6A**).

Since NPA blocks auxin efflux and causes accumulation of auxin within cells, the actual effect might be an accumulation of auxin due to reduced efflux. If this idea is correct, one would predict that a mild treatment with NPA combined with addition of low concentrations of the polar transportable auxin indole-3-acetic acid (IAA) in non-transformed BY-2 cells should phenocopy the effect of a high concentration of NPA. I therefore tested what happened, when non-transformed cells were treated by a combination of a low (3 μM) concentration of NPA with a low (2 μM) concentration of IAA. This combined treatment resulted in a conspicuous loss of division synchrony mimicking the effect of a high (12 μM) concentration of NPA (**Fig. 6B**).

These data show that, in this cell line, the pattern of cell division depends on polar auxin flow within the cell file (despite the overall presence of 0.9 μM of the artificial auxin 2,4-dichlorophenoxyacetic acid (2,4-D) in the medium). The synergistic effect of low concentrations of NPA with low concentrations of IAA indicate that the intracellular accumulation of IAA is responsible for the reduced synchrony in response to the phytohormone NPA.

► **Figure 6:** Manipulation of synchrony by 12 μM TIBA (compared to the untreated sample) (**A**), a combined treatment with 3 μM NPA and 2 μM IAA (compared to the effect of 12 μM NPA and the untreated sample) (**B**), and 2 μM NAA (compared to the effect of 2 μM IAA and the untreated sample) (**C**). Frequency distribution over cell number per file is shown for non-transformed BY-2 cells (**A**, **B**) and BY-2 cells overexpressing YFP-mT (**C**) at day 4 after inoculation. Each distribution is based on 3000 individual cells from three independent experimental series. Error bars indicate SE.

Figure 6



3.1.2 The actin filaments are constitutively bundled in a BY-2 cell line overexpressing YFP-talin

To better understand the role of actin in auxin-dependent patterning, I searched for a situation, where actin filaments were constitutively bundled. For this purpose, a transgenic BY-2 cell line was generated by stable transformation with a fusion between the yellow fluorescent protein (YFP) and the actin-binding domain of mouse talin (mT) under control of a 35S promoter.

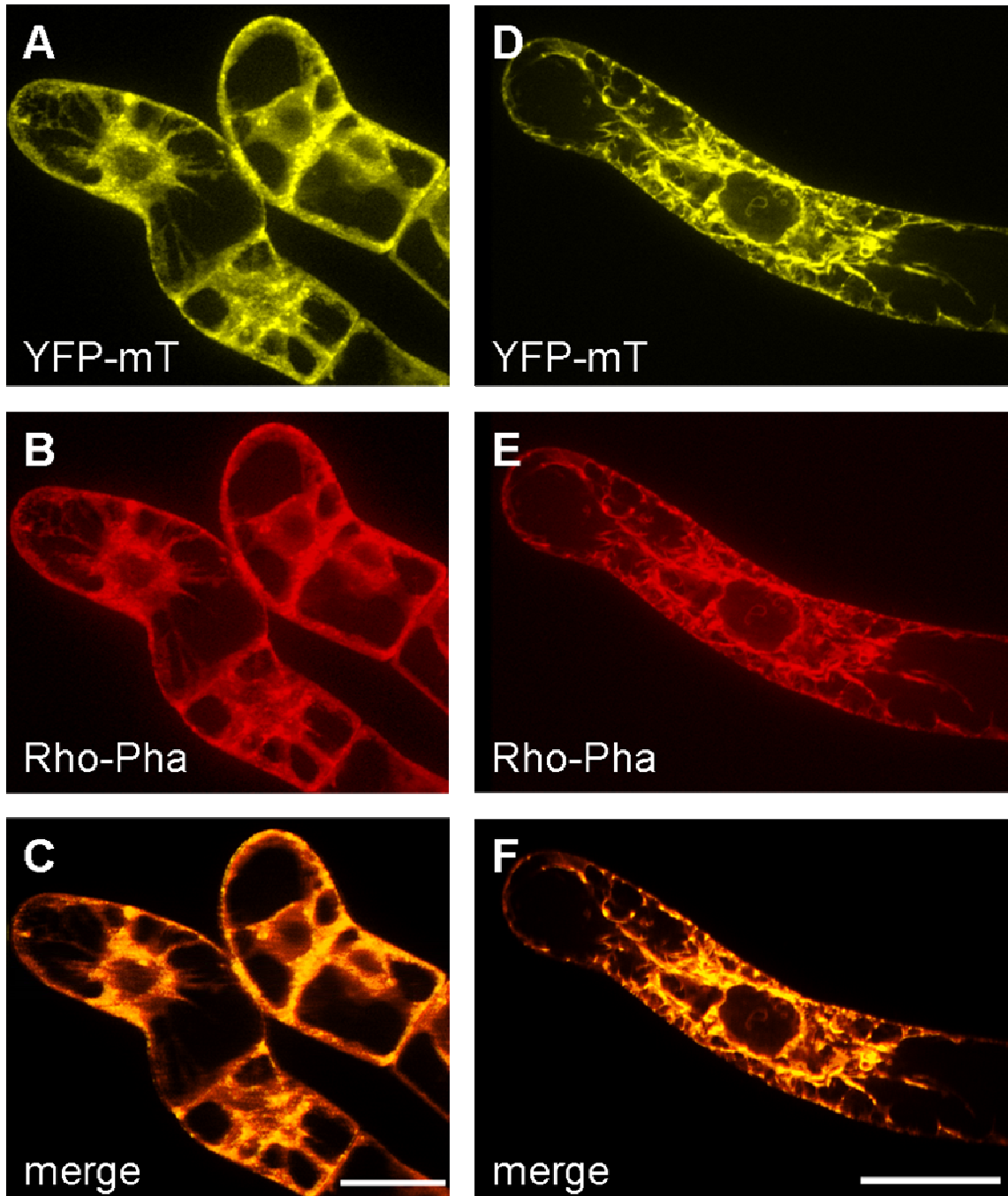
If the excess of YFP-mT fusion would cause a constitutive bundling of actin filaments, it should be possible, by means of the YFP-mT line, to manipulate auxin-dependent patterning through the altered organisation of actin in this cell line.

I therefore compared the arrangement of actin filaments in non-transformed control cells with cells overexpressing YFP-mT (**Figs. 7 and 8**). The actin cytoskeleton was visualised either in non-transformed BY-2 cells by the rhodamine-phalloidin staining method or, in case of the BY-2 YFP-mT line, observed directly *in vivo*.

To confirm that YFP-mT binds to and visualises actin filaments, BY-2 cells overexpressing the fusion protein were also co-stained with rhodamine-phalloidin after gentle permeabilisation. Patterns of yellow YFP-fluorescence and red rhodamine-phalloidin fluorescence emitted from double-labelled BY-2 cells were essentially identical (**Fig. 7**), showing that YFP-mT binds to the entire actin cytoskeleton in a specific manner.

► **Figure 7:** Co-localisation of YFP-mT and of rhodamine-phalloidin in BY-2 cells overexpressing YFP-mT in the absence (**A-C**) or in the presence (**D-F**) of 2 μ M IAA. YFP-mT fluorescence (**A, D**). Rhodamine-phalloidin fluorescence (**B, E**). **C, F** Merged fluorescences of (**A**) and (**B**) or (**D**) and (**E**), respectively. Orange colour indicates areas where the images overlap and where the two markers co-localise. Bars = 20 μ m.

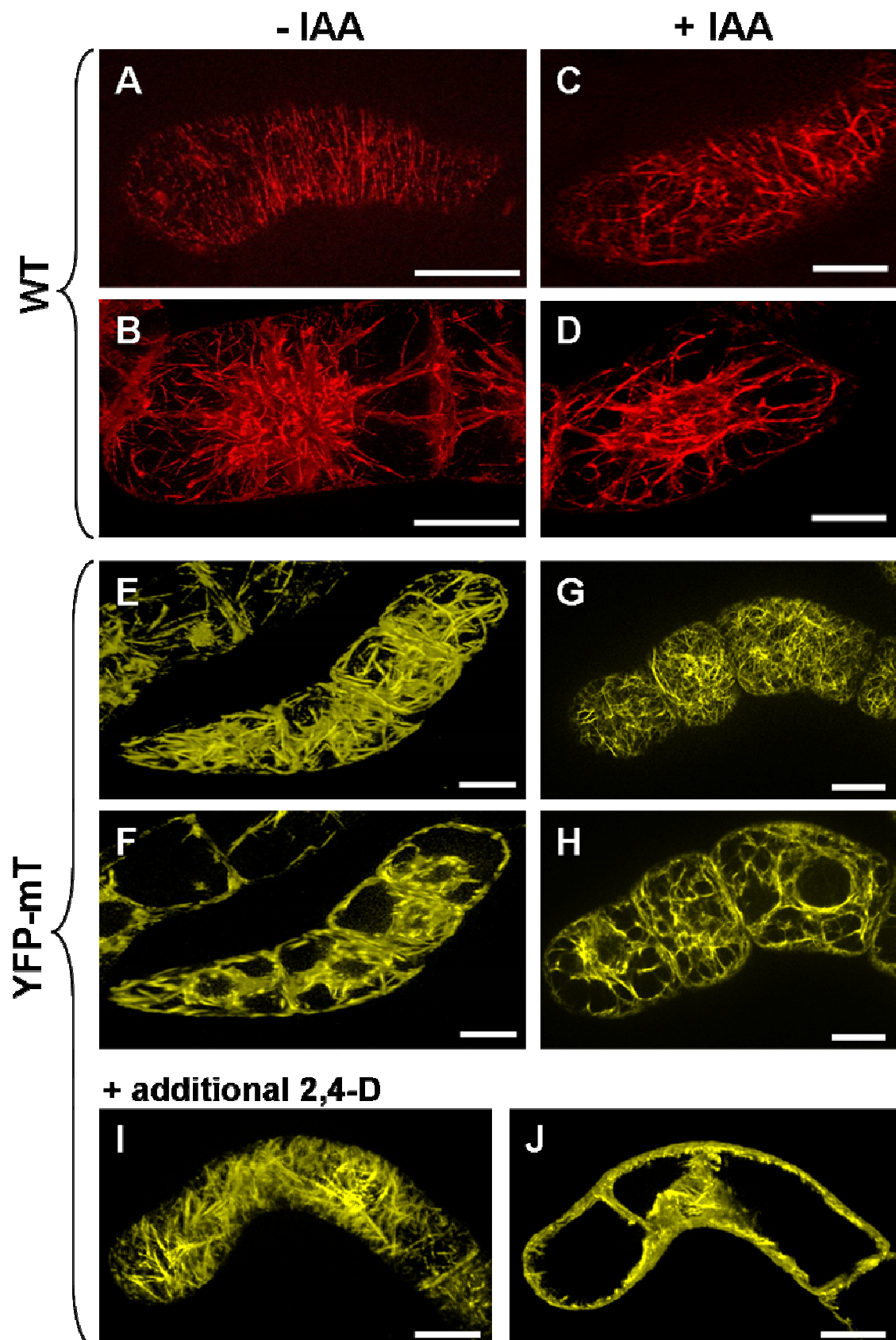
Figure 7



The non-transformed BY-2 cells displayed a fine network of transversely oriented actin filaments in the cortical region (**Fig. 8A**). Prominent fine actin filaments were also visible around the nucleus and radially oriented in transvacuolar strands (**Fig. 8B**). In contrast, actin was heavily bundled in cells overexpressing YFP-mT both in the cortical (**Fig. 8E**) and in the perinuclear regions (**Fig. 8F**). These observations demonstrate that the overexpression of the actin-binding domain of mouse talin indeed induced a strong reorganisation of the actin cytoskeleton.

► **Figure 8:** Actin filaments in non-transformed BY-2 cells (WT, **A-D**), visualised by TRITC-phalloidin in comparison with cells overexpressing YFP-talin (YFP-mT, **E-J**) in the absence (**A, B, E, F**) and the presence (**C, D, G, H**) of 2 μ M IAA or in the presence of additional 2 μ M 2,4-D (**I, J**). For each cell, a focal section in the cortical (**A, C, E, G, I**) and in the central (**B, D, F, H, J**) region is shown. Bars = 20 μ m.

Figure 8



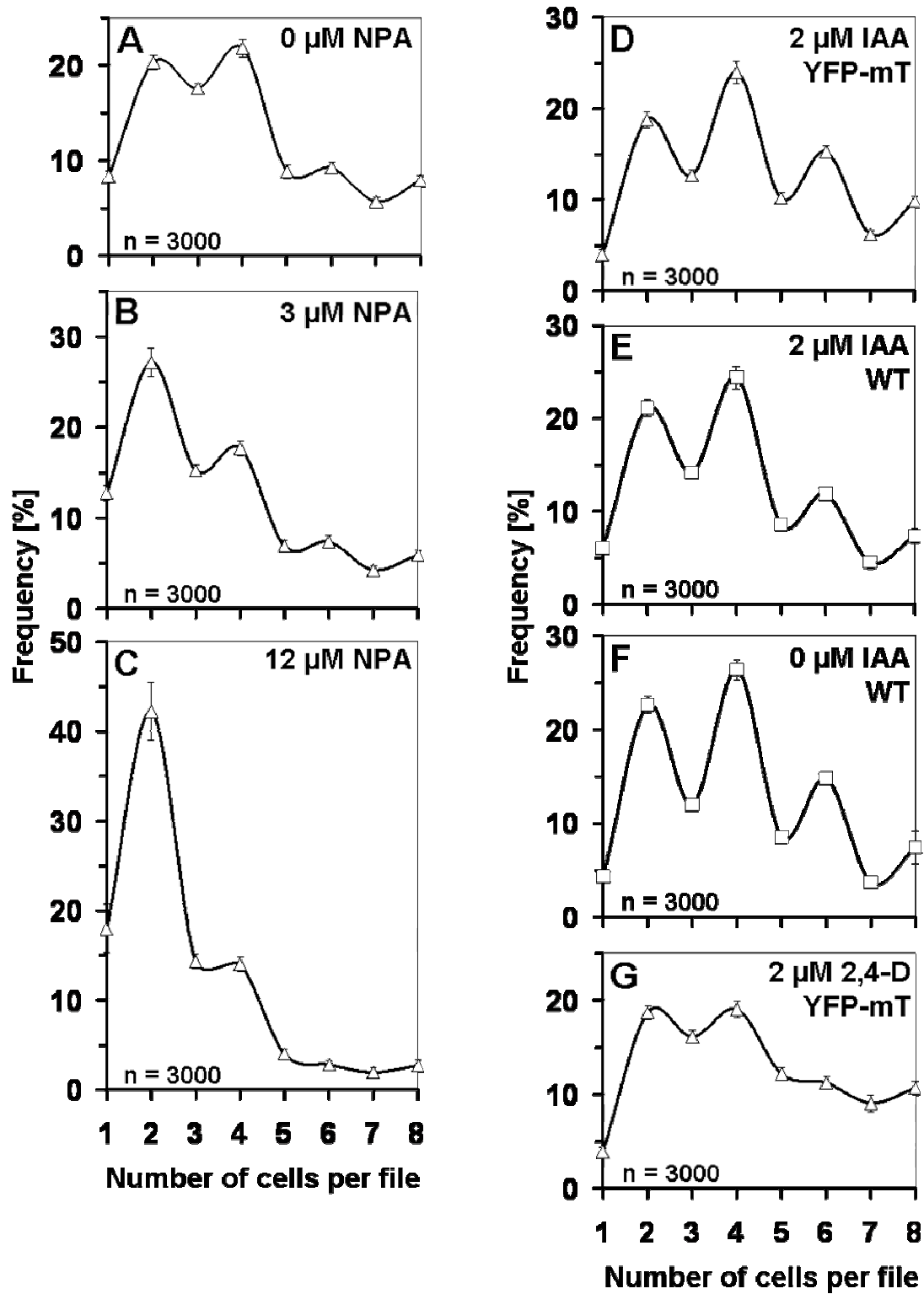
3.1.3 The synchrony of cell division is affected by bundling of actin

With exception of a small delay and a somewhat reduced amplitude of the division response, the global temporal pattern of cell division in the YFP-mT line was comparable to that in the non-transformed BY-2 cell line (**Fig. 5A**, p. 31). However, the synchrony of cell division was affected in the YFP-mT line (**Fig. 9A**). The characteristic oscillatory behaviour typical for the non-transformed control is hardly detectable. In other words, the difference in the incidence of files with even and uneven cell numbers is strongly reduced in YFP-mT cells. This difference was persistent, when the selective pressure on the cell line was relieved by omitting hygromycin from the medium, suggesting that it is an effect of the transgene and not an effect of the selection pressure.

I further investigated how the pattern of cell division responded to treatment with NPA. Similar to the non-transformed BY-2 cell line, the frequency peaks for higher cell numbers disappeared progressively (**Fig. 9, B and C**). Generally, the YFP-mT cell line appeared to be affected more readily as compared to the non-transformed cell line. Already for 12 μM NPA files with more than two cells had become very rare (**Fig. 9C**), whereas in the non-transformed cell line a higher concentration (30 μM NPA) was required to cause a similar effect (**Fig. 5E**, p. 31). Conversely, the effect of 3 μM NPA in the YFP-mT cell line was comparable to that observed in the non-transformed cell line upon addition of 12 μM NPA.

► **Figure 9:** Frequency distribution over cell number per file in BY-2 cells overexpressing YFP-talin at day 4 after inoculation in the absence of NPA (**A**), in the presence of 3 (**B**) or 12 μM NPA (**C**) or upon supplementation with 2 μM IAA (**D**) or additional 2 μM 2,4-D (**G**). As a control the response of non-transformed (WT) cells to 2 μM IAA (**E**) is shown in comparison to the distribution in the absence of IAA (**F**). Each distribution is based on 3000 individual cells from three independent experimental series. Error bars indicate SE.

Figure 9



Moreover, cell division was more impaired (**Fig. 5, F1 and F2**, p. 31) and cell elongation was more elevated (**Fig. 5G1**) at 12 μM NPA in the YFP-mT cell line as compared to the non-transformed cell line. Since viability at 30 μM NPA was strongly reduced in the YFP-mT cell line (in contrast to the non-transformed cell line), it was not possible to measure cell division responses for the transgenic line (for details, see **Appendix**, p. 92).

In summary, already low concentrations of NPA caused effects in the YFP-mT cell line that were observed in the non-transformed cell line only for higher concentrations of this inhibitor. In other words, the YFP-mT line is, *in sensu strictu*, more sensitive to NPA as compared to the non-transformed BY-2 cell line.

These data show that the synchrony of cell division is already *a priori* strongly deteriorated as compared to the non-transformed cell line. This goes along with an elevated sensitivity of cell division to NPA. Thus, the constitutive bundling of actin filaments in the YFP-mT line was accompanied by an impaired synchrony in auxin-dependent patterning.

3.1.4 The synchrony of cell division can be restored by polar transportable auxins

If the observed correlation between constitutively bundled actin and impaired synchrony of cell division is the manifestation of a causal relationship, one would predict that the synchrony should be restored, when the microfilament bundles are replaced by a configuration with finer, detached actin filaments. To test this prediction, I tried to generate detached microfilament strands by adding supplementary auxins. The BY-2 cells overexpressing YFP-talin were cultivated either upon addition of the auxins indole-3-acetic acid (IAA) or 1-naphthyl acetic acid (NAA) that are both polarly transported, or the same concentration of 2,4-dichlorophenoxyacetic acid (2,4-D). The auxin 2,4-D is, at least in tobacco cells,

not secreted by the efflux carrier responsible for polar auxin flow (Delbarre et al. 1996; Paciorek et al., 2005).

The presence of IAA leads to a debundling of actin both in the cortical region and around the nucleus. In contrast to the massive actin bundles characteristic for the IAA-free sample (**Fig. 8, E and F**, p. 37), numerous fine cortical actin filaments were observed upon addition of 2 μ M IAA (**Fig. 8G**), and even the transvacuolar strands were much finer than in the untreated control (**Fig. 8H**). This auxin effect was specific for IAA. When 2 μ M 2,4-D was added (in addition to the 0.9 μ M of 2,4-D that was present in all samples), this had no effect on the arrangement of actin filaments (**Fig. 8, I and J**).

How did these hormone treatments affect the pattern of cell division in the YFP-mT line? After addition of IAA, the synchrony of cell division, manifest as characteristic pattern with elevated frequencies of even-numbered cell files, was restored in the YFP-mT cell line (**Fig. 9D**, p. 39). In contrast, additional 2,4-D just shifted the frequency distribution towards higher cell numbers without restoring the synchrony. The residual difference in the frequencies of even and uneven cell numbers was even lower than in the untreated control line (compare **Fig. 9G** to **Fig. 9A**). When the response of non-transformed control cells to IAA was investigated, I did not see any significant change of synchrony. The only effect consisted in a slight shift of the distribution to higher cell numbers (compare **Fig. 9E** to **Fig. 9F**). In contrast, a treatment with 2 μ M NAA was able to rescue the synchrony of cell division partially (**Fig. 6C**, p. 33). However, NAA was clearly less effective than IAA.

Summarising these results, I observed that actin filaments were constitutively bundled in a BY-2 line overexpressing YFP-talin. This bundling of actin interferes with the synchrony of cell division in such a way that the division pattern is affected. Addition of polarly transported auxins, but not an increase of auxin *per se*, could restore both a normal organisation of actin and the synchrony of cell division.

3.2 Localisation of the actin-nucleation factor ARP3

To understand how the orientation of actin filaments is related to the polar patterning of cell division in the BY-2 cell line, I searched for a molecular marker for actin-nucleation sites. After cloning the tobacco homologue of ARP3, a member of the nucleating ARP2/3 complex, I studied its localisation *in vivo* during patterned cell division in BY-2 cells.

3.2.1 Isolation of tobacco ARP3

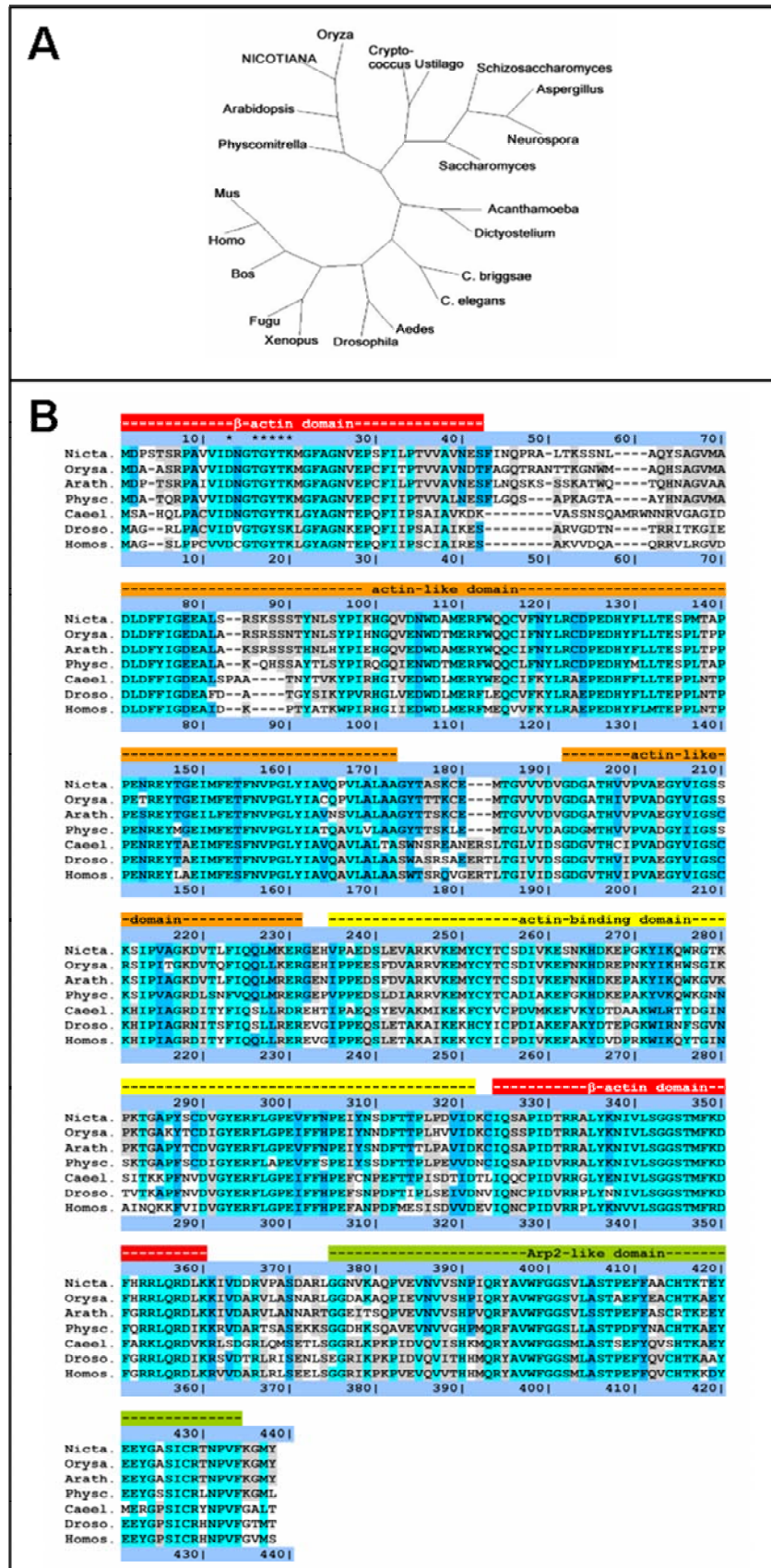
A full-length cDNA for tobacco *Arp3* was isolated by RT-PCR using total mRNA from tobacco BY-2 cells as a template. The primers were designed based on alignments of known plant *Arp3* sequences. The resultant coding sequence of *Arp3* was kindly provided by Dr. J. Fišerová, (Department of Botany, Faculty of Science, Charles University Prague, Czech Republic).

The obtained sequence coded for a protein consisting of 428 amino-acid residues that were highly homologous to ARP3 from *Arabidopsis thaliana* (EMBL accession number AY093149), *Oryza sativa* (EMBL accession number AP004092, 428 amino acids), or *Physcomitrella patens* (EMBL accession number AM287016, 424 amino acids). A phylogenetic tree was constructed for the most closely related homologues (identified by a BLAST search using the peptide sequence as query) based on the neighbour-joining method (Saitou and Nei, 1987). This tree showed that the *bona-fide* tobacco ARP3 sequence clustered with the other plant ARP3 sequences to a separate branch of the tree (**Fig. 10A**). The alignment of the corresponding peptide sequences (**Fig. 10B**) confirmed the high degree of conservation between the tobacco sequence and known ARP3 sequences from other organisms. The similarity is not confined to a high conservation of all the domains that could be identified, but extends even to sequence details. For instance, the sequence motif DxGTGYTK (**Fig. 10B**, *asterisks*) that has been associated with nucleotide binding (Beltzner and

Pollard, 2004) is conserved in the tobacco sequence. The high conservation to known ARP3 sequences and the presence of the relevant domains and motives strongly suggests that the cloned sequence represents the tobacco homologue of ARP3.

► **Figure 10:** Phylogenetic analysis and alignment of the protein sequences of *Nicotiana tabacum* ARP3 and homologues from other organisms. **A** A phylogenetic tree of *Nicotiana tabacum* ARP3 and variant ARP3 from diverse organisms based on the neighbour-joining method (Saitou and Nei, 1987). **B** Alignment of the deduced amino-acid sequences of ARP3 from *Nicotiana tabacum*, *Oryza sativa*, *Arabidopsis thaliana*, *Physcomitrella patens*, *Caenorhabditis elegans*, *Drosophila melanogaster* and *Homo sapiens*. The alignment was created using the ClustalW program (<http://www.ebi.ac.uk/clustalw/index.html>) and coloured by residue conservation according to Lassmann and Sonnhammer (2005). The lines above the alignment indicate the conserved regions of ARP3. The *asterisks* label the putative nucleotide binding sequence motif (Beltzner and Pollard, 2004).

Figure 10

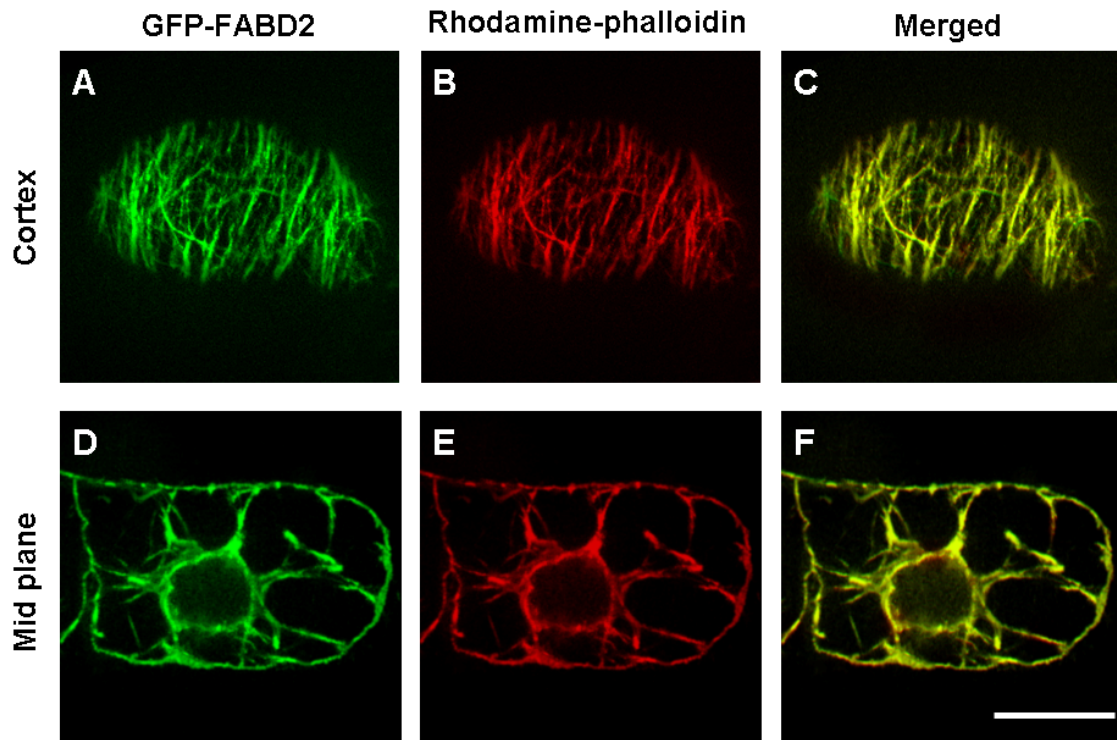


3.2.2 Visualisation of actin filaments by stable GFP-fimbrin expression

The second actin-binding domain (ABD2) of the *Arabidopsis thaliana* fimbrin 1 protein (AtFim1) was fused to the C-terminus of the green fluorescent protein (GFP) and stably expressed in tobacco BY-2 cells to generate the BY-2 GFP-FABD2 cell line. Projections of optical sections revealed GFP fluorescence of filamentous structures near the cell cortex and along cytoplasmic strands at the mid plane. To ensure that these structures did represent actin filaments, rhodamine-phalloidin staining was performed after gentle permeabilisation of the cells with glycerol. The filamentous structures labelled by GFP and the rhodamine fluorescence were completely congruent (**Fig. 11**), demonstrating that the GFP-fimbrin ABD2 fusion protein labelled actin filaments in tobacco BY-2 GFP-FABD2 cells.

► **Figure 11:** Visualisation of actin filaments by stably expressed GFP-FABD2 and by rhodamine-phalloidin in tobacco BY-2 cells. GFP-FABD2 fluorescence (**A, D**), rhodamine-phalloidin fluorescence (**B, E**), and merged signal (**C, F**) in focal sections of the cortical region (**A-C**) or the mid plane (**D-F**) of a BY-2 GFP-FABD2 cell. Yellow colour in the merged images (**C, F**) indicates areas where the two markers co-localise. Bars = 20 μm .

Figure 11



3.2.3 Localisation of actin-nucleation sites upon transient expression of RFP-ARP3 in BY-2 GFP-FABD2 cells

For transient expression of actin-related protein 3 (ARP3), the coding sequence of full length *Nicotiana tabacum Arp3* was inserted into a transient expression vector resulting in an N-terminal fusion of ARP3 to the red fluorescent protein (RFP-ARP3).

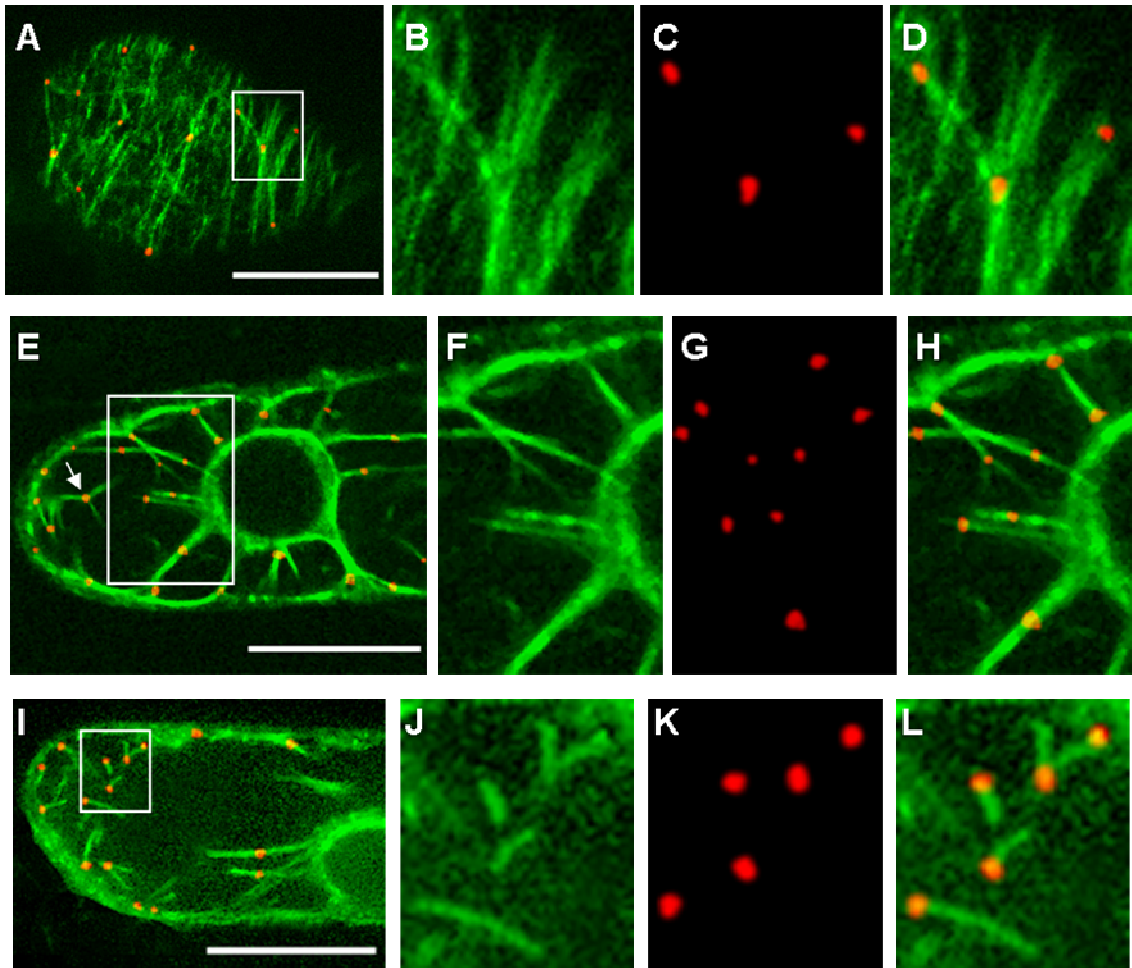
The localisation of RFP-labelled ARP3 proteins was analysed in BY-2 GFP-FABD2 cells upon particle bombardment with this construct using projections of serial optical sections. The ARP3 signals appeared as distinct dots and clearly decorated all arrays of the actin cytoskeleton, namely cortical microfilaments, the perinuclear network and the transvacuolar strands (**Fig. 12**). The dots were also frequently found at points of actin-filament branching (for instance **Fig. 12E**, *white arrow*).

To test whether the ARP3 dots correspond to sites of actin filament nucleation, Latrunculin B (Lat B) was used as a tool to specifically eliminate actin filaments. A treatment with 500 nM LatB for 10 h removed the actin cytoskeleton completely, as far as could be judged from epifluorescence microscopy. However, when the inhibitor was washed out, new actin structures (short filaments, Y-shaped junctions) reappeared within 15 min emerging from the labelled ARP3 dots (**Fig. 12, I-L**).

A similar subcellular distribution of ARP3 was observed in cells that recovered from cold treatment after cold-induced, reversible degradation of actin filaments for 10 h at 2°C (data not shown). The subcellular distribution of the ARP3 dots was not affected neither by LatB nor by cold (data not shown).

► **Figure 12:** Transiently expressed RFP-ARP3 decorates actin filaments in tobacco BY-2 cells that stably express GFP-FABD2. **A-D** Co-localisation of RFP-ARP3 and GFP-FABD2 in a focal section of the cortical region. **E-H** Co-localisation of RFP-ARP3 and GFP-FABD2 in a focal section of the perinuclear region with cytoplasmic strands. **I-L** Localisation of RFP-ARP3 during the recovery of actin filaments after Latrunculin B treatment (500 nM, 10 h). Details boxed in **A**, **E** and **I** are shown in **B**, **F** and **J** for the GFP-FABD2 fluorescence, in **C**, **G** and **K** for the RFP-ARP3 fluorescence, and in **D**, **H** and **L** for dual fluorescence, respectively. The arrow in panel **E** exemplarily highlights a site of actin-filament branching. Bars = 20 µm.

Figure 12



3.2.4 ARP3 is enriched in the distal halves of terminal cells

The results described above (3.1, pp. 28ff) demonstrated that the organisation of actin filaments is important for patterned cell division in BY-2 cells implicating that, amongst other factors, the polarity of microfilaments is responsible for divisional patterning.

To gain insight into the role of microfilament polarity in the context of cell-file polarity, the RFP-ARP3 construct was now used as a marker for *bona-fide* sites of actin nucleation.

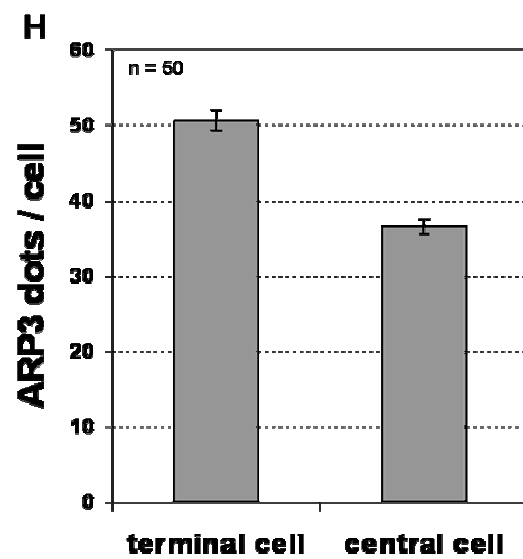
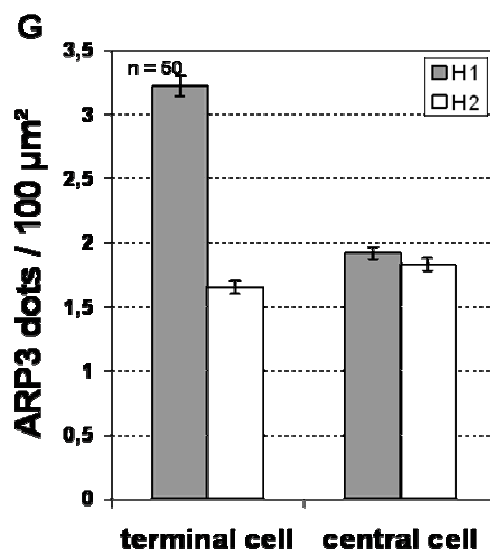
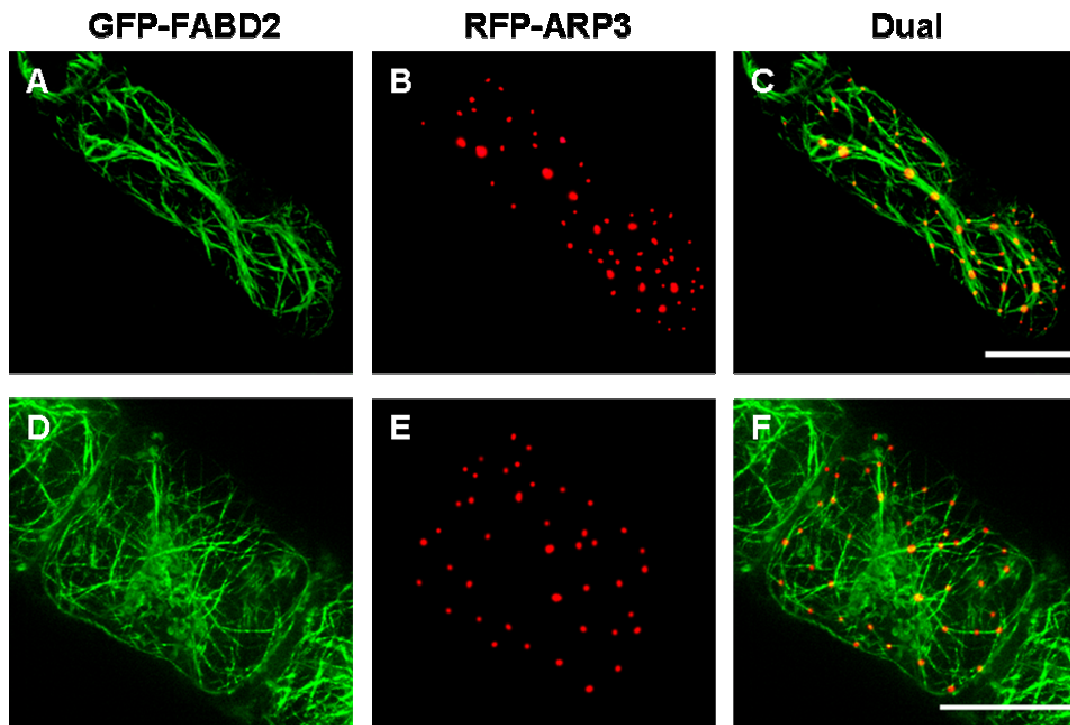
For this purpose, the distribution of ARP3 dots either in terminal or in central cells of a given cell file was analysed (Fig. 13).

To determine the areal densities, the maximum projections from serial stacks of terminal or central cells were subdivided into distal and proximal halves (Fig. 13G, *H1* and *H2*, respectively), and the ARP3 dots were scored over the cross-sectional area in the central plane of the cells. Hereby, the cross-sectional area occupied by the nucleus was subtracted, because in this region the cytoplasm was almost completely filled such that the density of ARP3 dots was very low. Since the nucleus is relatively large, this inhomogeneity might distort the quantification and even produce (artefactual) gradients if compared to the nuclear-free regions.

The distribution of ARP3 was dependent on the cell type. Whereas the density ranged around 1.8 ARP3 dots per 100 μm^2 in both halves of central cells or in the proximal halves of terminal cells, it was strongly (to 3.2 ARP3 dots per 100 μm^2) increased in the distal halves of terminal cells. As a consequence, the total number of dots per cell was increased by almost 40% in terminal over central cells (Fig. 13H). This means that additional ARP3 dots are formed in the distal half of terminal cells.

► **Figure 13:** Distribution of RFP-ARP3 sites in terminal (A-C) *versus* central (D-F) cells in the GFP-FABD2 cell line. The GFP-FABD2 signals are shown in A and D, the RFP-ARP3 signals in B and E, and the dual fluorescence in C and F, respectively. Bars = 20 μm . G Areal densities of ARP3 dots in distal (*H1*) or proximal (*H2*) halves of terminal *versus* central cells. H Total number of ARP3 dots per cell in terminal *versus* central cells. The values in G and H represent in each case averages from 50 individuals collected from 32 independent transient transformations. Error bars indicate SE.

Figure 13



3.2.5 Behaviour of ARP3 and PIN1 during divisional patterning

To test for possible correlations between ARP3 (as marker for actin nucleation) and PIN1 (as marker for cell polarity) during divisional patterning, I followed the localisation of both markers through the formation of axial, pluricellular files in the BY-2 cell line (**Fig. 14**). ARP3 was again visualised by a RFP fusion transiently expressed in the GFP-FABD2 background. PIN1 (from *Arabidopsis thaliana*) was visualised as fusion with GFP under control of the homologous PIN1 promoter (Benková et al., 2003).

In the unicellular state, symmetric single cells could be distinguished from asymmetric single cells. Whereas RFP-ARP3 was homogeneously distributed in symmetric cells (**Fig. 14, A and B**), the density of ARP3 dots was clearly increased in one cell half of unicellular asymmetric files (**Fig. 14, D and E**). The PIN1 signal was localised at the periphery of the cells. Plasmolysis experiments (data not shown) suggested that the signal was confined to the plasma membrane. In contrast to the ARP3 signal, PIN1 was found to be uniformly distributed during the unicellular state, irrespective of whether the cells were symmetric (**Fig. 14C**) or asymmetric (**Fig. 14F**).

In bicellular files, the density of the ARP3 signal was increased in the distal halves of both cells compared to their proximal halves (**Fig. 14, G and H**). The PIN1 signal was clearly concentrated at the (newly deposited) cross wall (**Fig. 14I**).

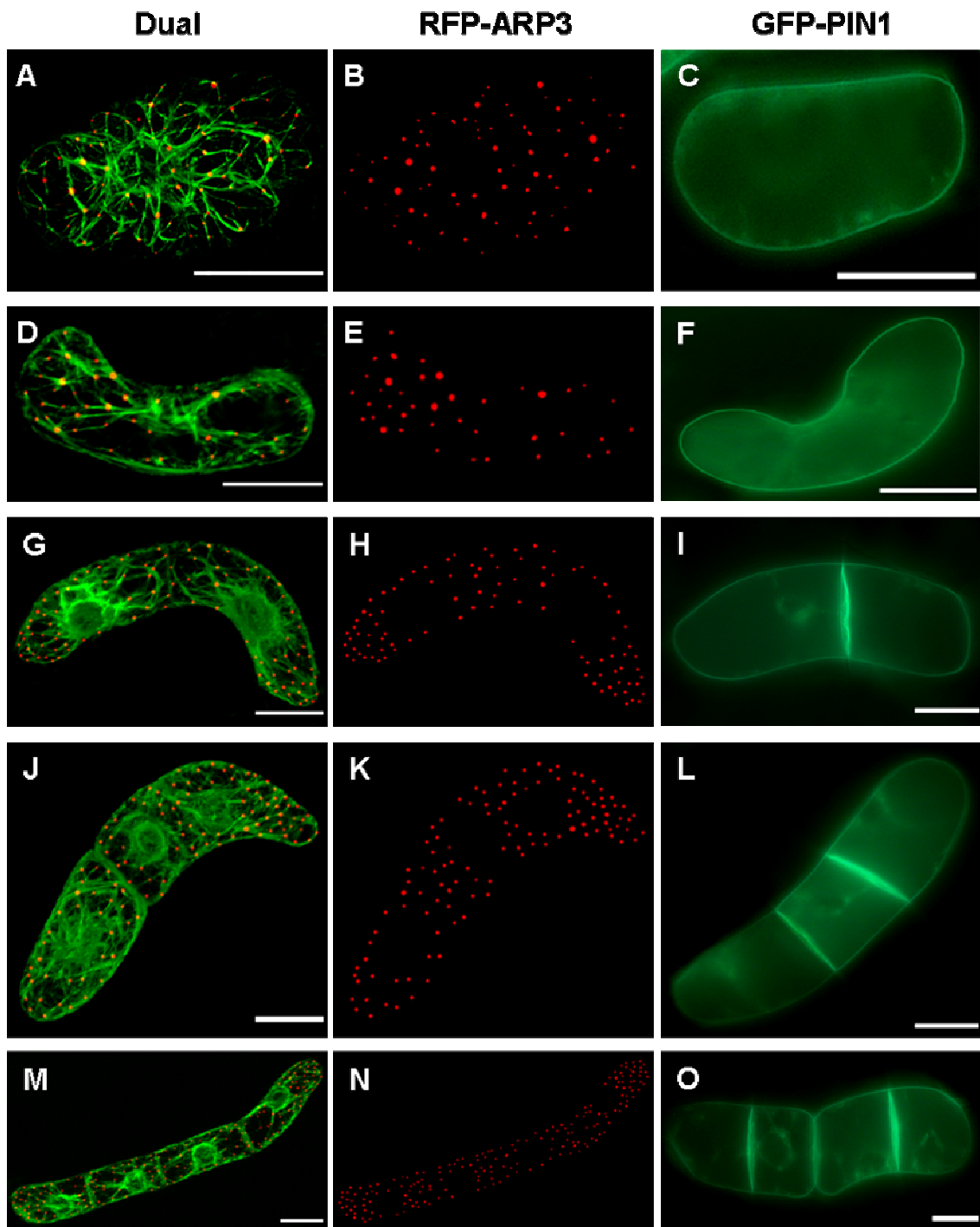
Tricellular files occur less frequently than bi- or quadricellular files (**3.1.1, Fig. 5B**, p. 31). These tricellular files result from an asymmetric first division, followed by a second division of the larger daughter cell that thus is “younger” as compared to the opposite terminal cell (data not shown). In these tricellular files, ARP3 was exclusively enriched in distally located half of the “younger” terminal cell (**Fig. 14, J and K**). Again, PIN1 was concentrated in the cross

walls. However, the signal was strongest in the most recent cross wall belonging to the “younger” terminal cell (**Fig. 14L**).

In quadricellular files, the ARP3 signal was enriched in the distal halves of both terminal cells but equally distributed within the central cells (**Fig. 14, M and N**). The PIN1 signal was still concentrated in the cross walls, but the signal was most intense in the cross walls belonging to the two terminal cells. In contrast, the signal was comparably faint in the cross walls located more centrally in the file. In many quadricellular files, disintegration of the file into smaller subsets became detectable (**Fig. 14O**).

► **Figure 14:** Dynamic redistribution of ARP3 and PIN1 during axial division of BY-2 cells. Dual visualisation of actin microfilaments by GFP-FABD2 and RFP-ARP3 (**A, D, G, J, M**). The distribution of ARP3 (**B, E, H, K, N**) and PIN1 (**C, F, I, L, O**) is shown for the symmetric unicellular (**A-C**), the asymmetric unicellular (**D-F**), the bicellular (**G-I**), the tricellular (**J-L**), and the quadricellular (**M-O**) state. Bars = 20 μ m.

Figure 14



3.3 Summary

To get insight into the role of actin for auxin transport, patterned cell division was used to monitor the polarity of auxin fluxes in the tobacco cell line BY-2. Cell divisions in BY-2 cell files were synchronised, leading to higher frequencies of files with even cell numbers as compared to files with uneven cell numbers. This synchrony could be perturbed by inhibitors of polar auxin transport (NPA, TIBA).

To address the role of actin in this synchrony, a bundled configuration of the actin cytoskeleton was induced by overexpressing mouse talin. The bundling of actin impaired the synchrony of cell division and increased the sensitivity to NPA. Addition of polarly transported auxins (IAA, NAA), but not auxin *per se* (2,4-D), restored both the normal organisation of actin and the synchrony of cell division.

In order to analyse the role of microfilament polarity in the context of patterned cell division, tobacco *Arp3* was cloned and a RFP-ARP3 construct was used as a marker for sites of actin nucleation. These actin-nucleation sites were localised *in vivo* in transgenic BY-2 cells stably expressing GFP-FABD2 which labels actin filaments. ARP3 decorated actin filaments and was significantly enriched in the distal halves of terminal tobacco cells.

Thereafter, the behaviour of ARP3 and PIN1 (as a marker for cell polarity) was investigated during the formation of pluricellular BY-2 cell files. The strongest PIN1 signals were concentrated at the newly deposited cross walls emerging during the latest cell divisions in terminal cells of the files. In bicellular and quadricellular files the density of ARP3 was clearly increased in both poles of the files, whereas in the tricellular state the ARP3 dots were exclusively enriched in the distal half of the "younger" terminal cell. In contrast to PIN1 that was uniformly distributed in the plasma membrane of single cells, the ARP3 localisation depended on the symmetry of the unicellular state.

4. Discussion

Pattern formation in plants typically occurs in a situation, where new elements are continuously added during the patterning process. This raises the question how the pattern of cell division in tobacco BY-2 cells is induced and maintained over time, when the number of cells in a file increases progressively. Thus, cell division is of special interest, because cell polarity - and possibly microfilament polarity as well – must be *de-novo* generated or at least reamplified, when a new cell pole is formed during division.

In the following, I shall first discuss the role of actin in the maintenance of polar patterning in the BY-2 cell line. The second part deals with the role of actin polarity (monitored by the actin-nucleation factor ARP3) for the polarity of auxin flow, culminating in a model on generation and maintenance of cell polarity during patterned cell division.

4.1 Actin is involved in auxin-dependent patterning

4.1.1 Auxin synchronises cell divisions in BY-2 cells

Cell division in the BY-2 line follows a clear pattern with elevated frequencies of files composed of an even number of cells (**Fig. 5B**, p. 31). This type of division pattern had been previously shown in a different tobacco cell line (Virginia Bright Italia 0, VBI-0) to result from weak coupling between the divisions of neighbouring cells (Campanoni et al., 2003). This coupling was dependent on polar auxin flux and displayed a clear unidirectionality. Since VBI-0 derives from a specific tissue (stem pith parenchyma) this pattern might represent a peculiar feature of this cell line. Unfortunately, VBI-0 was found to be recalcitrant to stable transformation. However, the results described above (**3.1.1**, pp. 28ff)

clearly demonstrate that patterning can be also analysed in the widely used BY-2 cell line, where a panel of numerous fluorescent marker lines is available.

A mild inhibition of polar auxin transport, which only slightly affects the rate of cell division (**Fig. 5, F1 and F2**, p. 31) and leaves cell elongation unaffected (**Fig. 5G1**), equalises the prevalence of files with even cell numbers (**Fig. 5C**). This effect is not only induced by NPA, but also by other phytohormones (such as TIBA, **Fig. 6A**, p. 33). The actual signal seems to be the intracellular accumulation of IAA produced by these phytohormones. I infer this from the synergistic effect of low concentrations of IAA with low concentrations of NPA (**Fig. 6B**). This leads to the conclusion that polar intrafile auxin transport, and not auxin *per se*, is responsible for the patterning of cell division in BY-2 cells.

These experiments confirmed that the BY-2 cell line is a suitable system to study auxin-dependent patterning of cell division, because the degree of division synchrony can be used as physiological indicator for the efficiency of polar auxin transport.

4.1.2 Generation of constitutively bundled actin by overexpression of mouse talin

In the next step, I asked for the role of actin in the generation of this pattern. Previous studies have shown that the auxin response to actin involves changes in the bundling of actin filaments, with bundled actin being characteristic for a situation, where auxin was depleted (Waller et al., 2002; Holweg et al., 2004). These changes of actin organisation feed back to the sensing and/or processing of auxin (Waller et al., 2002; Nick, 2006). I therefore searched for approaches to manipulate the bundling of actin filaments.

Although the expression of fluorescent proteins fused to actin binding domains has been used as a convenient tool to study the actin cytoskeleton in living

cells, the dynamics and organisation of filamentous actin may change due to the expression of the fusion protein. These changes may cause problems with transport or signalling processes that regulate cell division and cell growth. As published by Ketelaar et al. (2004), the overexpression of mouse talin can impair actin dynamics to some degree by inhibiting the actin-depolymerising activity of actin-depolymerising factor (ADF) resulting in a bundling of actin filaments.

I used mouse talin overexpression to induce a constitutive bundling of actin filaments thus mimicking a situation usually observed upon auxin depletion. For this purpose, a transgenic BY-2 cell line overexpressing YFP-mT under control of the 35S promoter was established. In order to eliminate transformants with low expression activity, a stringent selection regime was applied. This resulted in a generally high level of expression leading to a very strong bundling of actin filaments (**Fig. 8, E and F**, p. 37). This bundling was also shown by Kost et al. (1998) in growing tobacco pollen tubes using high expression levels of GFP-mouse talin. When actin was stained by rhodamine-phalloidin in the cells overexpressing YFP-mT, both signals were found to be congruent (**Fig. 7**, p. 35), demonstrating that the entire pool of filamentous actin is visualised by YFP-mT in a specific manner.

4.1.3 Actin bundling impairs the auxin-dependent synchrony

By means of the YFP-mT cell line, it was now possible to show that the bundling of actin interferes with the auxin-dependent synchrony of cell division. As a consequence of the impaired coordination of the cell cycle, the difference in the incidence of files with even and uneven cell numbers was already strongly reduced in untreated YFP-mT cells (**Fig. 9A**, p. 39), an effect that could be even enhanced by treatment with NPA, an inhibitor of polar auxin flux. Already low concentrations of NPA produced alterations in the frequency distribution that were observed in the non-transformed cell line only for higher concentrations of

this inhibitor. For instance, already for 12 μM NPA files with more than two cells had become very rare. In the non-transformed cell line, a higher concentration (30 μM NPA) was required to cause a similar effect (compare **Fig. 9C**, p. 39, to **Fig. 5E**, p. 31). In other words, the NPA sensitivity was increased in the YFP-mT cell line. This was also evident, when overall division activity was plotted over the concentration of NPA (**Fig. 5, F1 and F2**).

This means that NPA and YFP-mT interfere in a multiplicative manner with the coupling signal, indicating that both factors target to the same signalling cascade. Most certainly, the increased sensitivity to NPA in the YFP-mT line implies that the link between actin organisation and synchrony of cell division is based on changes of directional auxin transport.

4.1.4 Polarly transportable auxins restore the synchrony of the division pattern

If this reasoning is correct, and the constitutively bundled actin as well as the impaired synchrony of cell division depend on polar auxin transport, this synchrony should be restored, when the massive actin bundles in the YFP-mT line are replaced by a finer meshwork of detached microfilament strands. This prediction was tested experimentally by supplementing the medium either with polarly transported auxins (IAA, NAA) or 2,4-D, which is not excreted by the efflux carrier responsible for polar auxin flux (Delbarre et al., 1996; Paciorek et al., 2005). I tested, whether these auxins are able to generate detached microfilament strands. Consistent with previous studies of maize and rice coleoptiles (Waller et al., 2002; Holweg et al., 2004), IAA (but not 2,4-D) induced a dissociation of actin bundles and a formation of fine microfilament strands (**Fig. 8, G and H**, p. 37). The debundling of actin might be explained by the upregulation of auxin-responsive ADF genes as previously described for grape stem cuttings (Thomas and Schiefelbein, 2002).

The synchrony of cell division characterised by elevated frequencies of even-numbered cell files was restored in the YFP-mT line after addition of IAA (**Fig. 9D**, p. 39) and, to a lesser extent, of NAA (**Fig. 6C**, p. 33). In contrast, additional 2,4-D had no effect on the affected synchrony of cell division in the YFP-mT line. Thus, when actin is organised in fine strands, cell division is synchronous. When actin is bundled (as a consequence of constitutive expression of YFP-mT), the synchrony is impaired. When the fine actin strands are recovered upon addition of polarly transportable auxins (rather than auxin *per se*), this results in a rescue of division synchrony. In other words, the fine strands of actin are both, necessary and sufficient for the synchrony of cell division.

4.1.5 Auxin controls its own transport by modulating the organisation of actin filaments

Several studies have linked the polarity of auxin transport to actin-dependent vesicle flow (for review see Friml, 2003; Nick, 2006). For instance, the cycling of the auxin-efflux factor PIN1 between intracellular compartments and the plasma membrane could be affected by the actin inhibitor Cytochalasin D or treatment with Brefeldin A (Steinmann et al., 1999), a fungal toxin that inhibits the budding of vesicles. BFA treatment results not only in the bundling of cortical actin filaments, but also shifts the dose-response of auxin-dependent growth towards higher concentrations of auxin (Waller et al., 2002). Conversely, inhibition of myosins by 2,3-butanedione monoxime (BDM) impairs auxin-dependent cell division in the tobacco cell line VBI-0 (Holweg et al., 2003).

The scope of this dissertation was to investigate whether the bundling of actin will impair the polarity of auxin flux monitored by using the synchrony of cell division as a marker.

The experiments by Geldner et al. (2001) have shown that actin is involved in the localisation of auxin-efflux factors. The present work extends these observations. It is not only actin *per se* that is necessary for polar transport of

auxin. It is a specific organisation of actin that is required. The fine cortical actin filaments observed in the non-transformed cell line are necessary for the patterning of cell division. This patterning process is dependent on polar auxin flux as to be concluded from the impaired synchrony of cell division in the YFP-mT line and the increased NPA-sensitivity of this cell line. Addition of polar transportable auxin (IAA), but not auxin *per se* (2,4-D), can restore the fine cortical actin filaments and, as well, the synchrony in YFP-mT cells resulting in an ordered pattern of cell divisions, where files with even cell numbers are more frequent than files with uneven cell numbers. Thus, the fine cortical actin filaments are sufficient for polar patterning in the background of this cell line. In other words, this study provides evidence for a feedback loop between polar auxin flux and the organisation of the actin cytoskeleton. Auxin is therefore able to control its own transport by altering the organisation of actin filaments.

4.2 What controls the asymmetric cycling of the auxin-efflux carrier?

The findings discussed above (4.1, p. 55) demonstrate that the organisation of actin filaments is important for auxin-dependent, patterned cell division in tobacco BY-2 cells, implicating that the polarity of microfilaments guide the patterning process via the transport of auxin-signalling components. Since the asymmetric localisation of the auxin-efflux carrier (PIN1 and other factors) seems to be driven by actin, it is necessary to search for factors that control the polarity of microfilaments.

To follow the auxin-dependent pattern over time, it is essential to use markers that uncover the role of microfilament polarity in conjunction with cell-file polarity. For this purpose, ARP3 was used as marker for microfilament polarity *in vivo*.

4.2.1 Actin organisation and directional auxin flow

To gain insight into the role of microfilament polarity for the induction and maintenance of cell-file polarity, tobacco ARP3 was cloned and fused to RFP resulting in a RFP-ARP3 construct.

Biolistic, transient transformation of tobacco BY-2 cells overexpressing GFP-FABD2 with this construct allowed simultaneous visualisation of ARP3 proteins and the actin cytoskeleton in living cells. The RFP-labelled ARP3 was found to specifically decorate all arrays of the actin cytoskeleton.

After recovery from transient elimination of actin filaments (by Latrunculin B or cold), the regenerated filaments emerged from sites that were marked by ARP3 proteins (**Fig. 12I**, p. 48). This recovery experiments clearly showed that ARP3 marked the sites of actin-filament nucleation consistent with published immunofluorescence studies using antibodies against ARP3 and actin (Fišerová et al., 2006).

The abundance of the ARP3 signal was significantly increased in the apical half of the terminal cells of a given file (**Fig. 13G**, p. 50). This observation is in line with immunolocalisation studies in tip growing plant cells, where elements of the ARP2/3 complex were enriched at the sites of polar growth (Van Gestel et al., 2003; Hable and Kropf, 2005). Thus, it points to a role of actin-related proteins in the establishment of cell polarity.

The PIN1 protein fused to GFP was predominantly localised to the plasma membranes of the cross walls, resembling the distribution observed in the root elongation zone of *Arabidopsis thaliana* (for review, see Friml, 2003). However, this localisation was not uniformly found in all cells of a file. It was again the terminal cells, where the PIN1 signal was clearest and mostly confined to the cross wall (**Fig. 14O**, p. 53). In the more central cells, the PIN1 signal was progressively fading away. Although the role of PIN1 for auxin efflux is not completely understood, it is now generally accepted as reliable marker for the direction of auxin flux (e.g. during primordia formation in the apical meristem, Reinhard et al., 2003). Since the polar distribution of PIN1 is most conspicuous in the terminal cells, it can be inferred that the polarity of auxin flux is most

pronounced in those cells and expressed to a lesser extent in the central cells of a file. One observation should be emphasised in this context: upon disintegration of a cell file, PIN1 redistributes such that it is found uniformly along all cell walls, the former cross wall as well as the side walls (**Fig. 14, C and F**, p. 53). This would indicate that auxin efflux is temporarily delocalised in these single cells.

4.2.2 A model on actin polarity and auxin fluxes during polar patterning

Using ARP3 as marker for actin nucleation and PIN1 as marker for the polarity of auxin flux, it is possible to construct a model on the generation and perpetuation of cell polarity during patterned cell division in BY-2 cells (**Fig. 15**). This model assumes that pluricellular files consist of two cell types that differ with respect to polarity:

1. The two terminal cells of a file are clearly polar with PIN1 concentrated at the proximally located cross wall and ARP3 concentrated at the distally located cell pole (**Fig. 15, state 0**). Upon disintegration of the file into single cells, the graded distribution of ARP3 seems to persist, whereas PIN1 is redistributed uniformly over the plasma membrane of these cells (**Fig. 15, state 1A**). The first division of these terminal cells is asymmetrical separating a polar tip cell (in the following defined as “apical” cell) from an apolar “basal” cell (**Fig. 15, state 1B**). However, this situation is short-lived, because the apical cell will soon divide giving rise to a tricellular situation (**Fig. 15, state 1C**). In contrast to the two basal cells of the tricellular file, where ARP3 is uniformly distributed, the apical cell maintains polarity marked by a polar distribution of ARP3. PIN1 is concentrated at the proximal cross wall of the apical cell, but progressively fading out from the (older) cross wall that separates the two basal cells. When a quadricellular file is produced by an additional division of one of the basal cells (**Fig. 15, state 1D**), a polarity becomes

manifest in the “basal”, terminal cell: ARP3 is observed to be more abundant in the terminal half of this cell and PIN1 strongly accumulates at the proximal cross wall, such that the initial situation (**Fig. 15, state 0**) is restored.

2. The fate of the apolar, central cells differs. They do not exhibit a graded distribution of the ARP3 signal, and the accumulation of PIN1 at the cross wall is much fainter as compared to the terminal cells, indicating that they are caused by residual amounts of PIN1 laid down during the preceding (polar) ancestors of these cells. Upon disintegration, ARP3 is still uniformly distributed, and the same holds true for PIN1 (**Fig. 15, state 2A**). These apolar cells divide symmetrically giving rise to a bicellular file (**Fig. 15, state 2B**), where subsequently polarity becomes manifest in both daughter cells (**Fig. 15, state 2C**): PIN1 is concentrated in the cross wall, whereas ARP3 is focussed to the terminal halves of these cells. The two cells divide simultaneously in an asymmetric fashion, whereby the bulk of the ARP3 signal is assigned to the terminal daughter cell (**Fig. 15, state 2D**). Again, the initial situation (**Fig. 15, state 0**) is restored, however, by passing through different initial states.

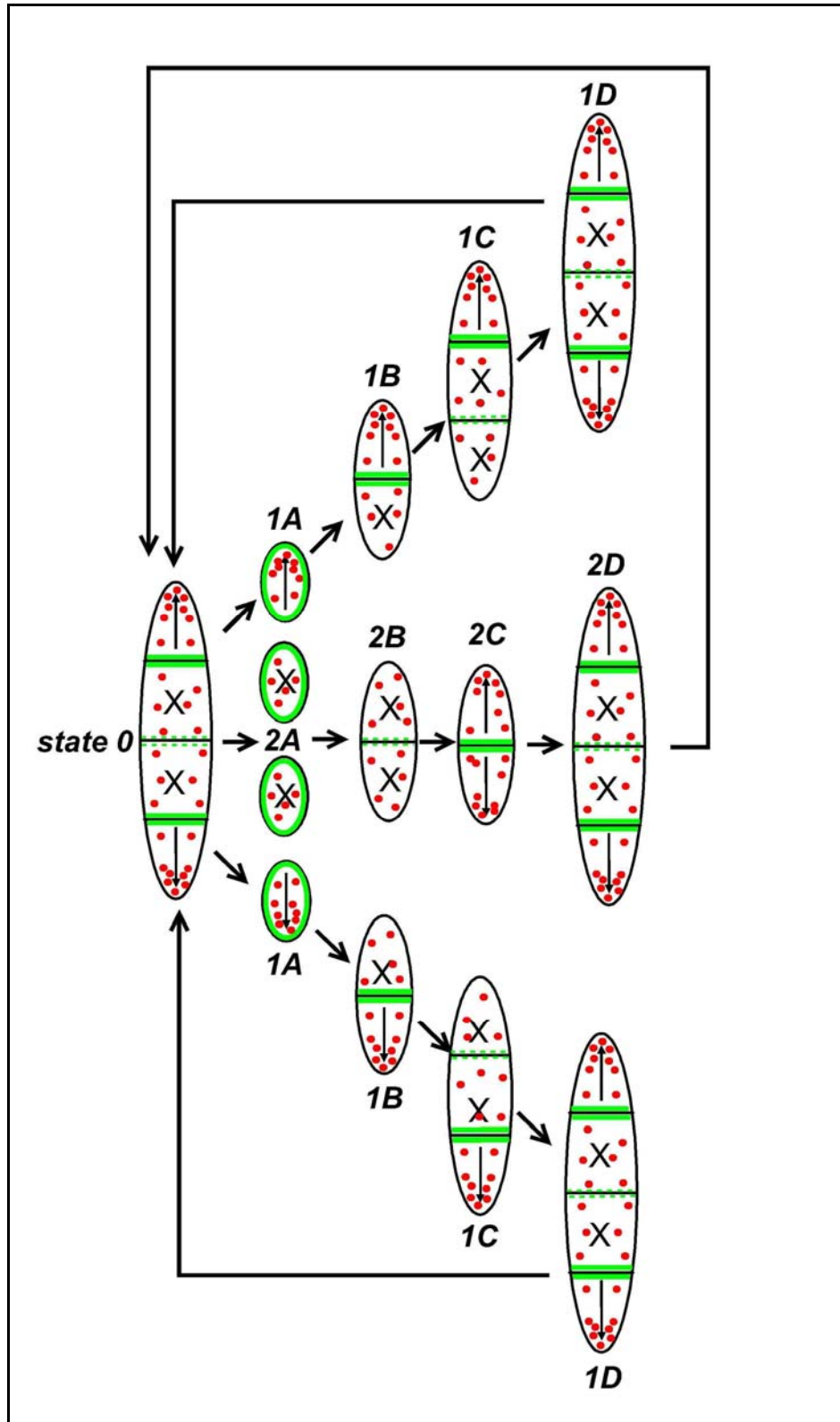


Figure 15: Model for the generation and perpetuation of cell polarity during patterned cell division in BY-2 cells. Pluricellular files consist of polar cells (*arrow*) and apolar cells (*X*). The distribution of ARP3 (*red dots*) and the localisation of PIN1 (*green lines*) are depicted in colour. The different states during divisional patterning are described in section 4.2.2.

The model suggests that ARP3 is a more persistent marker of cell polarity than PIN1. This can be concluded from the finding that the ARP3 gradient is conserved in the terminal half of polar cells upon disintegration of the file, whereas PIN1 is evenly spread over the plasma membrane. If this reasoning is correct, ARP3 is involved in the positioning of auxin efflux carriers by nucleating actin filaments, which in turn serve as tracks for the vesicle-trafficking machinery. In other words, ARP3 might represent a direct manifestation of cell polarity.

Recent studies link the auxin-signalling machinery to the organisation of actin (for review, see Xu and Scheres, 2005). Vesicle trafficking mediated by ADP-ribosylation factors (ARFs) is required for the polar localisation of Rho-related GTPases in plants (ROPs) which control regulators of the ARP2/3 complex (Frank et al., 2004). On the other hand, ARF-mediated vesicle trafficking also control the localisation of PIN proteins which is known to rely on the activity of the serine-threonine kinase PINOID (PID; Friml et al., 2004) and on the function of P-glycoproteins (PGP)/multiple drug resistance (MDR) proteins (Noh et al., 2001). However, the initial cues for the polar localisation of ROP and PIN proteins remain unknown.

These studies suggest that ARF-dependent vesicle flow controls actin nucleation (activity of the ARP2/3 complex) and the multifaceted membrane-localisation patterns of PIN proteins in parallel. However, the finding that ARP3 marks cell polarity more persistently than PIN1, which is redistributed during the single-cell state, suggests that the actin cytoskeleton is acting upstream of PIN1 localisation. This could be due to actin-dependent movement of the vesicles that deliver the auxin-efflux carriers to the plasma membrane or to actin-dependent tethering of these carriers in the plasma membrane. Thus, there appear to be two ways, how ARFs control the localisation of PIN1: directly, by controlling the budding of vesicles that carry the auxin-efflux carriers, and indirectly, by modulation of ROP proteins that in turn control regulators of the ARP2/3 complex. The resulting changes of actin nucleation will alter the organisation of actin filaments and, in consequence, the actin-dependent transport and/or tethering of the auxin-efflux carriers.

An additional regulatory feature of this model should be emphasised. The clearly polar, terminal cell in *state 1B* (**Fig. 15**, p. 64) inhibits the initiation of a “new” polarity in its immediate proximity. The inhibitory field only ranges from the polar, terminal cell to the next but one cell within the tricellular file (**Fig. 15, state 1C**).

Such a process is known as lateral inhibition and occurs between the elements within the patterned field that mutually compete for a limiting factor. It contains qualitative decisions which are probably brought about by autocatalytic feedback loops. This type of mechanism has been demonstrated in auxin-dependent patterning for the positioning of lateral organs called phyllotaxis (Reinhardt et al., 2000) and for the venation in developing leaves (Sachs, 2000), latter culminating in the widely expected auxin-canalisation model (**1.3, Fig. 2**, p. 6).

Most certainly, the inhibitory signal, which acts as limiting factor and suppresses the regeneration of an additional pole in BY-2 cell-file formation, might be the flux of auxin, i.e. the polar, terminal cell will transport more auxin than its apolar neighbour cell thus depleting it from auxin. It was recently shown that auxin can inhibit the endocytotic step of the constitutive cycling of PIN proteins (Paciorek et al., 2005). The biological significance of this process was demonstrated for PIN2 in the gravitropic response of roots. Here, auxin accumulates at the new lower side of the gravistimulated root tip. As to be expected, PIN2 endocytosis is decreased at the lower side of the gravistimulated root, where the auxin concentration is increased, but continues on the upper, auxin-depleted side.

Thus, auxin increases levels of PIN proteins at the plasma membrane and concomitantly promotes its own efflux from cells providing a molecular mechanism for a positive feedback loop.

4.3 Conclusion

Polar transport of auxin has been identified as a central element of pattern formation. The polarity of auxin transport is linked to the cycling of *pin-formed* (PIN) proteins, a process that is related to actomyosin-dependent vesicle traffic.

In the present work, patterned cell division in tobacco BY-2 cells was used to monitor the polarity of auxin fluxes. In this cell line, single cells can be induced to develop pluricellular files with a clear axis.

Moreover, the division of individual cells within those files is synchronised by polar auxin flux leading to a prevalence of files composed of even cell numbers. This synchronous division pattern disappears, when the polarity of auxin transport is affected by treatment with inhibitors of polar auxin flux. Thus, the degree of division synchrony can be used as physiological indicator for the efficiency of polar auxin transport.

This system was utilised as a tool to analyse the impact of actin filaments on polar auxin flux during patterned cell division. By overexpression of the actin-binding protein talin, it was possible to induce excessive bundling of actin filaments in a transgenic BY-2 cell line. In these transformants, the synchrony of cell division was impaired in such a way that the pattern of cell division was affected.

However, by addition of transportable auxins (but not auxin *per se*), a normal organisation of actin could be restored in these cells. In parallel, a regular pattern of cell division was induced by transportable auxins.

Thus, the organisation of actin filaments is crucial for optimal auxin transport, indicating that auxin controls its own transport by changing the state of actin filaments within a self-amplifying feedback loop.

To gain insight into the role of microfilament polarity in the context of cell-file polarity, a RFP-ARP3 construct was used as a marker for *bona-fide* sites of actin nucleation.

By simultaneous visualisation of actin and ARP3 in living cells, it was demonstrated that ARP3 decorates actin filaments. When actin filaments were transiently eliminated and then allowed to recover, ARP3 marked the sites from which the new filaments emanated. The density of ARP3 was increased in the apex of terminal tobacco BY-2 cells.

The distribution of the ARP3 signal over the cell files was compared with the localisation of PIN1 culminating in a model for patterned cell division which comprises auxin transport, actin cytoskeleton and cell polarity. This model is based on the assumption that pluricellular BY-2 files are composed of two cell types which can be categorised according to their polarity. In contrast to the apolar cell, the polar cell remains its polarity upon disintegration of the file and suppresses the polarisation of the adjacent cell by short-ranged lateral inhibition during early cell-file formation. When the cell file disintegrates into single cells, the polar distribution of PIN1 is temporarily lost in the polar cells. However, the intracellular gradient of ARP3 persists. The working hypothesis assumes that this ARP3 gradient is involved in the reinduction of a polar PIN1 distribution and thus in the reestablishment of the polar auxin flux which will synchronise the division of daughter cells.

4.4 Outlook

The present doctoral thesis has led to some exciting questions relating to auxin signalling, actin organisation and cell polarity during patterned cell division of BY-2 cells. Future work might therefore focus on the following aspects:

1. A better knowledge of the relationship between auxin and actin-associated proteins should provide new insights on the question how auxin signalling is coupled to actin bundling. Unlike other actin-binding proteins, actin-depolymerising factor (ADF) interacts with both filamentous and globular actin, and either drives filament turnover or

induces depolymerisation. Thus, it is anticipated that altering ADF levels will have dramatic effects on the regulation of actin dynamics. For example, the overexpression of ADF disrupts cytoplasmic filamentous actin cables and reduces the expansion of polar-growing root hairs. In contrast, the antisense inhibition of ADF produces an increase in the density of cytoplasmic filamentous actin and excessive expansion of root hairs (Dong et al., 2001). Based on the findings of this dissertation, it will be important to work towards an understanding of how ADF and probably other actin-binding proteins regulate actin organisation with respect to auxin signalling. Is the debundling of actin in the YFP-mT BY-2 cell line observed in response to polarly transportable auxins related to the upregulation of auxin-responsive ADF genes?

2. Many of the components involved in auxin-dependent cell polarisation have been identified during the recent years, and first pathways that link regulators to cytoskeletal elements have emerged. Vesicle trafficking plays a central role in the establishment of cell polarity, but the specific controls of this process need to be revealed. In addition, the nature of the primary polarity cues remains unknown. ARP3 is concentrated in the tip of polar BY-2 cells, but the way how ARP3 is transported to the cell pole needs to be uncovered, for example by analysis of ARP3 localisation during mitosis and cell plate formation, i.e. when a new daughter cell is generated.
3. A still unsolved problem is the question how a plant cell is able to perceive an auxin flow as a signal. The observation that the rate of auxin transport can be increased several times by auxin itself, i.e. that auxin stimulates its own transport, is actually quite old. Starting with the pioneering work of Hertel and Flory (1968), this finding culminates in the idea that the potential auxin-efflux carrier represents “the real” auxin sensor. In other words, the stimulus is not a local auxin level, but the transport of auxin, more precisely, the amount of auxin which is polarly pumped to the apoplast by means of the auxin-efflux carrier. A very

recent methodological advance might shed light on the crucially important mechanisms of auxin sensing. So called caged derivatives of the transportable, natural auxin indole-3-acetic acid were synthesised that can be preloaded to plant cells and released by a laser pulse (Hayashi and Kusaka, unpublished). By combination of this approach with auxin-responsive reporters that allow to visualise the local activity of auxin, it should be possible to follow over time the response of patterned cell division in BY-2 cell files to a source of auxin, which is confined to one cell or even to one region of a cell. This would open the exciting possibility to study, for the first time in a physiological context, polar auxin transport on the cellular level.

5. Acknowledgments

The author thanks Dr. Federica Brandizzi (Research School of Biological and Molecular Sciences, Oxford Brooks University, UK) for the *p35S-YFP-talin* construct, Dr. Boris Voigt and Prof. Dr. Diedrik Menzel (Department of Plant Cell Biology, Institute of Cellular and Molecular Botany, University of Bonn, Germany) for the *pGFPm3abd2* construct, and Dr. Jindřiška Fišerová, (Department of Botany, Faculty of Science, Charles University Prague, Czech Republic) for the *psmGFP-ARP3* construct.

NPA was kindly provided by Dr. Wolfgang Michalke (Institute for Biology III, University of Freiburg, Germany). The BY-2 GFP-PIN1 tobacco cell line was kindly provided by Dr. Jan Petrášek (Institute of Experimental Botany, Academy of Sciences of the Czech Republic, Prague, Czech Republic).

This work was supported by a fellowship to Jan Maisch from the Landesgraduierten-Programm of the State of Baden-Württemberg and the German-Czech Scientific-Technical Cooperation program funded by the German Academic Exchange Service (DAAD).

6. References

An G (1985) High efficiency transformation of cultured tobacco cells. *Plant Physiol* **79**: 568-570

Beltzner CC, Pollard TD (2004) Identification of functionally important residues of Arp2/3 complex by analysis of homology models from diverse species. *J Mol Biol* **336**: 551-565

Benková E, Michniewicz M, Sauer M, Teichmann T, Seifertová D, Jürgens G and Friml J (2003) Local, efflux-dependent auxin gradients as a common module for plant organ formation. *Cell* **115**: 591-602

Berleth T, Sachs T (2001) Plant morphogenesis: long-distance coordination and local patterning. *Curr Opin in Plant Biol* **4**: 57–62

Bernard P, Couturier M (1992). Cell killing by the F plasmid CcdB protein involves poisoning of DNA-topoisomerase II complexes. *J Mol Biol* **226**: 735-745

Blanchoin L, Amann KJ, Higgs HN, Marchand JB, Kaiser DA, Pollard TD (2000) Direct observation of dendritic actin filament networks nucleated by Arp2/3 complex and WASP/Scar proteins. *Nature* **404**: 1007-1011

Brandizzi F, Snapp EL, Roberts AG, Lippincott-Schwartz J, Hawes C (2002) Membrane protein transport between the endoplasmic reticulum and the Golgi in tobacco leaves is energy dependent but cytoskeleton independent: evidence from selective photobleaching. *Plant Cell* **14**: 1293–1309

- Bünning E** (1965) Die Entstehung von Mustern in der Entwicklung von Pflanzen. In W Ruhland, ed, Handbuch der Pflanzenphysiologie (Vol. 15/1). Springer Verlag, Berlin, pp 383–408
- Bushman W, Thompson JF, Vargas L, Landy A** (1985). Control of directionality in lambda site specific recombination. *Science* **230**: 906-911
- Butler JH, Hu SQ, Brady SR, Dixon MW, Muday GK** (1998) *In vitro* and *in vivo* evidence for actin association of the naphthylphthalamic actin-binding protein from zucchini hypocotyls. *Plant J* **13**: 291-301
- Campanoni P, Blasius B, Nick P** (2003) Auxin transport synchronizes the pattern of cell division in a tobacco cell line. *Plant Physiol* **133**: 1251-1260
- Campbell RE, Tour O, Palmer AE, Steinbach PA, Baird GS, Zacharias DA, Tsien RY** (2002) A monomeric red fluorescent protein. *Proc Natl Acad Sci USA* **99**: 7877-7882
- Cande WZ, Goldsmith MH, Ray PM** (1973) Polar auxin transport and auxin-induced elongation in the absence of cytoplasmic streaming. *Planta* **111**: 279-296
- Chen R, Masson PH** (2006) Auxin transport and recycling of PIN proteins in Plants. In J Šamaj, F Baluška, D Menzel, eds, Plant endocytosis. *Plant Cell Monogr* (1), Berlin, pp 139-157
- Cholodny H** (1928) Beiträge zur hormonalen Theorie von Tropismen. *Planta* **6**: 118-134
- Darwin C, Darwin F** (1881) The power of movement in plants. D Appleton, New York

Delbarre A, Meller P, Imhoff V, Guern J (1996) Comparison of mechanisms controlling uptake and accumulation of 2,4-dichlorophenoxy acetic acid, naphthalene-1-acetic acid, and indole-3-acetic acid in suspension cultured tobacco cells. *Planta* **198**: 532-541

Dong CH, Xia GX, Hong Y, Ramachandran S, Kost B, Chua NH (2001) ADF proteins are involved in the control of flowering and regulate F-actin organization, cell expansion, and organ growth in *Arabidopsis*. *Plant Cell* **13**: 1333-1346

EI-Assal SD, Le J, Basu D, Saad ME, Mallery EL, Szymanski DB (2004) *DISTORTED2* encodes an ARPC2 subunit of the putative *Arabidopsis* ARP2/3 complex. *Plant J* **38**: 526-538

Finer JJ, Vain P, Jones MW, McMullen MD (1992) Development of the particle inflow gun for DNA delivery to plant cells. *Plant Cell Rep* **11**: 323–328

Fišerová J, Schwarzerová K, Petrášek J, Opartný S (2006) ARP2 and ARP3 are localized to sites of actin filament nucleation in tobacco BY-2 cells. *Protoplasma* **227**: 119-128

Frank M, Egile C, Dyachok J, Djakovic S, Nolasco M, Li R, Smith LG (2004) Activation of Arp2/3 complex-dependent actin polymerization by plant proteins distantly related to Scar/WAVE. *Proc Natl Acad Sci USA* **101**: 16379-16384

Friml J (2003) Auxin transport: shaping the plant. *Curr Opin in Plant Biol* **6**: 7–12

Friml J, Yang X, Michniewicz M, Weijers D, Quint A, Tietz O, Benjamins R, Ouwerk PB, Ljung K, Sandberg G, Hooykaas PJ, Palme K, Offringa R (2004) A PINOID-dependent binary switch in apical-basal PIN polar targeting directs auxin efflux. *Science* **306**: 862-865

Gälweiler L, Guan C, Müller A, Wisman E, Mendgen, Yephremov A, Palme K (1998) Regulation of polar auxin transport by AtPIN1 in *Arabidopsis* vascular tissue. *Science* **282**: 2226-2230

Geldner N, Anders N, Wolters H, Keicher J, Kronberger W, Müller P, Delbarre A, Ueda T, Nakano A, Jürgens G (2003) The *Arabidopsis* GNOM ARF-GEF mediates endosomal recycling, auxin transport, and auxin-dependent plant growth. *Cell* **112**: 219-230

Geldner N, Friml J, Stierhof YD, Jürgens G, Palme K (2001) Auxin transport inhibitors block PIN1 cycling and vesicle trafficking. *Nature* **413**: 425-428

Gierer A, Berking S, Bode H, David CN, Flick K, Hansmann G, Schaller H, Trenkner E (1972) Regeneration of hydra from reaggregated cells. *Nature* **239**: 98–101

Gierer A, Meinhard H (1972) A theory of biological pattern formation. *Kybernetik* **12**: 30–39

Hable WE, Kropf DL (2005) The Arp2/3 complex nucleates actin arrays during zygote polarity and growth. *Cell Mot Cytoskel* **61**: 9-20

Hartley JL, Temple GF, Brasch MA (2000). DNA cloning using *in vitro* site-specific recombination. *Genome Research* **10**: 1788-1795

Hertel R, Flory R (1968) Auxin movement in corn coleoptiles. *Planta* **82**: 123-144

Holweg C, Honsel A, Nick P (2003) A myosin inhibitor impairs auxin-induced cell division. *Protoplasma* **222**: 193-204

Holweg C, Süßlin C, Nick P (2004) Capturing *in vivo* dynamics of the actin cytoskeleton stimulated by auxin or light. *Plant Cell Physiol* **45**: 855-863

- Hou G, Kramer V, Wang Y, Chen R, Perbal G, Gilroy S, Blancaflor E** (2004) The promotion of gravitropism in *Arabidopsis* roots upon actin disruption is coupled with the extended alkalization of the columella cytoplasm and a persistent lateral auxin gradient. *Plant J* **39**: 113-125
- Jan YN, Jan LY** (2000) Polarity in cell division: What frames thy fearful asymmetry? *Cell* **100**: 599-602
- Kakimoto T, Shibaoka H** (1987) Actin filaments and microtubules in the preprophase band and phragmoplast of tobacco cells. *Protoplasma* **140**: 151–156
- Karimi M, De Mayer B, Hilson P** (2005) Modular cloning and expression of tagged fluorescent proteins in plant cells. *Trends Plant Sci* **10**: 103-105
- Karimi M, Inze D, Depicker A** (2002) Gateway vectors for *Agrobacterium*-mediated plant transformation. *Trends Plant Sci* **7**: 193-195
- Ketelaar T, Anthony RG, Hussey PJ** (2004) Green fluorescent protein-mTalin causes defects in actin organization and cell expansion in *Arabidopsis* and inhibits actin depolymerizing factor's actin depolymerizing activity *in vitro*. *Plant Physiol* **136**: 3990-3998
- Kost B, Spielhofer P, Chua NH** (1998) A GFP-mouse talin fusion protein labels plant actin filaments *in vivo* and visualizes the actin cytoskeleton in growing pollen tubes. *Plant J* **16**: 393-401
- Larkin JC, Marks MD, Nadeau J, Sack F** (1997) Epidermal fate and patterning in leaves. *Plant Cell* **9**: 1109-1120
- Lassmann T, Sonnhammer EL** (2005) Kalign - an accurate and fast multiple sequence alignment algorithm. *BMC Bioinformatics* **6**: 298, doi: 10.1186/1471-2105-6-298, <http://www.biomedcentral.com/1471-2105/6/298>

- Le J, El-Assal SD, Basu D, Saad ME, Szymanski DB** (2003) Requirements for *Arabidopsis* ATARP2 and ATARP3 during epidermal development. *Curr Biol* **13**: 1341-1347
- Li S, Blanchoin L, Yang Z, Lord EM** (2003) The putative *Arabidopsis* arp2/3 complex controls leaf cell morphogenesis. *Plant Physiol* **132**: 2034-2044
- Lomax TL, Muday GK, Rubery PH** (1995) Auxin transport. In PJ Davies ed, *Plant hormones: physiology, biochemistry, and molecular biology*. Kluwer, Dordrecht, pp 509-530
- Mathur J** (2005) The ARP2/3 complex: giving plant cells a leading edge. *BioEssays* **27**: 377-387
- Mathur J, Mathur N, Kernebeck B, Hülkamp M** (2003) Mutations in actin-related proteins 2 and 3 affect cell shape development in *Arabidopsis*. *Plant Cell* **15**: 1632-1645
- Mathur J, Spielhofer P, Kost B, Chua NH** (1999) The actin cytoskeleton is required to elaborate and maintain spatial patterning during trichome cell morphogenesis in *Arabidopsis thaliana*. *Development* **126**: 5559-5568
- Mattsson J, Sung ZR, Berleth T** (1999) Responses of plant vascular systems to auxin transport inhibition. *Development* **126**: 2979–2991
- Mayer U, Büttner G, Jürgens G** (1993) Apical-basal pattern formation in *Arabidopsis* embryos: studies on the role of the *gnom* gene. *Development* **117**: 149-162
- Meinhard H** (1976) Morphogenesis of lines and nets. *Differentiation* **6**: 117–123
- Meinhard H** (1986) The threefold subdivision of segments and the initiation of legs and wings in insects. *Trends Genet* **3**: 36–41

- Morris DA, Friml J, Zažímalová E** (2004) The transport of auxin. In PJ Davies, ed, *Plant hormones: biosynthesis, signal transduction, action*. Kluwer, Dordrecht, pp 437-470
- Mullins RD, Heuser JA, Pollard TD** (1998) The interaction of Arp2/3 complex with actin: nucleation, high affinity pointed end capping, and formation of branching networks of filaments. *Proc Natl Acad Sci USA* **95**: 6181-6186
- Murashige T, Skoog F** (1962) A revised medium for rapid growth and bioassays with tobacco tissue cultures. *Physiol Plant* **15**: 473-497
- Nagata T, Kumagai F** (1999) Plant cell biology through the window of the highly synchronized tobacco BY-2 cell line. *Methods Cell Sci* **21**: 123-127
- Nagata T, Nemoto Y, Hasezawa S** (1992) Tobacco BY-2 cell line as the “Hela” cell in the cell biology of higher plants. *Int Rev Cytol* **132**: 1–30
- Nick P** (2006) Noise yields order – auxin, actin, and polar patterning. *Plant Biol* **8**: 360-370
- Noh B, Murphy AS, Spalding EP** (2001) Multidrug resistance-like genes of *Arabidopsis* required for auxin transport and auxin-mediated development. *Plant Cell* **13**: 2441-2454
- Okada K, Ueda J, Komaki MK, Bell CJ, Shimura Y** (1991) Requirement of the auxin polar transport system in early stages of *Arabidopsis* floral bud formation. *Plant Cell* **3**: 677-684
- Olyslaegers G, Verbelen JP** (1998) Improved staining of F-actin and colocalization of mitochondria in plant cells. *J Microsc Oxford* **192**: 73–77

- Paciorek T, Zažimalová E, Ruthardt N, Petrášek J, Stierhof YD, Kleine-Vehn J, Morris DA, Emans N, Jürgens G, Geldner N, Friml J** (2005) Auxin inhibits endocytosis and promotes its own efflux from cells. *Nature* **435**: 1251-1256
- Petrášek J, Černá A, Schwarzerová K, Elčknér M, Morris DA, Zažimalová E** (2003) Do phytohormones inhibit auxin efflux by impairing vesicle traffic? *Plant Physiol* **131**: 254-263
- Phillips HJ** (1973) Dye exclusion tests for cell viability. In PF Kruse, MK Patterson, eds, *Tissue Cultures: Methods and Application*, Section VIII: Evaluation of Culture Dynamics. Academic Press, New York, p 406
- Raven JA** (1975) Transport of indoleacetic acid in plant cells in relation to pH and electrical potential gradients, and its significance for polar IAA transport. *New Phytol* **74**: 163-172
- Redig P, Shaul O, Inze D, Van Montagu M, Van Onckelen H** (1996) Levels of endogenous cytokinins, indole-3-acetic acid and abscisic acid during the cell cycle of synchronized tobacco BY-2 cells. *FEBS Lett* **391**: 175-180
- Reinhard D, Mandel T, Kuhlemeier C** (2000) Auxin regulates the initiation and radial position of plant lateral organs. *Plant Cell* **12**: 507–518
- Reinhardt D, Pesce ER, Stieger P, Mandel T, Baltensperger K, Bennett M, Traas J, Friml J, Kuhlemeier C** (2003) Regulation of phyllotaxis by polar auxin transport. *Nature* **426**: 255-260
- Robinson RC, Turbedsky K, Kaiser DA, Marchand JB, Higgs HN, Choe S, Pollard TD** (2001) Crystal structure of Arp2/3 complex. *Science* **294**: 1679-1684

- Rubery PH** (1990) Phytotropins: receptors and endogenous ligands. *Symp Soc Exp Biol* **44**: 119-146
- Rubery PH, Sheldrake AR** (1974) Carrier-mediated auxin transport. *Planta* **188**: 101-121
- Sachs T** (1993) The specification of meristematic cell orientation by leaves and by auxin. *Aust J Plant Physiol* **20**: 541-553
- Sachs T** (2000) Integrating cellular and organismic aspects of vascular differentiation. *Plant Cell Physiol* **41**: 649–656
- Saedler R, Mathur N, Srinivas BP, Kernebeck B, Hülkamp M, Mathur J** (2004) Actin control over microtubules suggested by *DISTORTED2* encoding the *Arabidopsis* ARPC2 subunit homolog. *Plant Cell Physiol* **45**: 813-822
- Saitou N, Nei M** (1987) The neighbor-joining method: a new method for reconstructing phylogenetic trees. *Mol Biol Evol* **4**: 406-25
- Spemann H** (1938) Embryonic development and induction. Yale University Press, New Haven
- Steinmann T, Geldner N, Grebe M, Mangold S, Jackson CL, Paris S, Gälweiler L, Palme K, Jürgens G** (1999) Coordinated polar localization of auxin efflux carrier PIN1 by GNOM ARF GEF. *Science* **286**: 316–318
- Sun H, Basu S, Brady SR, Luciano RL, Muday GK** (2004) Interactions between auxin transport and actin cytoskeleton in developmental polarity of *Fucus distichus* embryos in response to light and gravity. *Plant Physiol* **135**: 266-278

- Svitkina TM, Borisy GG** (1999) Arp2/3 complex and actin depolymerizing factor cofilin in dendritic organization and treadmilling of actin filament array in lamellipodia. *J Cell Biol* **145**: 1009-1026
- Sweeney BM, Thimann KV** (1937) The effect of auxin on cytoplasmic streaming. *J Gen Physiol* **21**: 123-135
- Szymanski DB, Marks MD, Wick SM** (1999) Organized F-actin is essential for normal trichome cell morphogenesis in *Arabidopsis*. *Plant Cell* **11**: 2331-2348
- Thimann KV, Reese K, Nachmikas VT** (1992) Actin and the elongation of plant cells. *Protoplasma* **171**: 151-166
- Thomas P, Schiefelbein J** (2002) Cloning and characterization of an actin depolymerizing factor gene from grape (*Vitis vinifera* L.) expressed during rooting in stem cuttings. *Plant Science* **162**: 283-288
- Thompson KS, Hertel R, Müller S, Tavares JE** (1973) 1-N-naphthylphthalamic and 2, 3, 5-triiodobenzoic acids: in vitro binding to particulate cell fractions and action on auxin transport in corn coleoptiles. *Planta* **109**: 337-352
- Turing AM** (1952) The chemical basis of morphogenesis. *Phil Trans R Soc London* **237**: 37-72
- Turner S, Sieburth LE** (2003) Vascular patterning. In CR Somerville, EM Meyerowitz, eds, *The Arabidopsis Book*. American Society of Plant Biologists, Rockville, doi: 10.1199/tab.0073, <http://www.aspb.org/publications/arabidopsis/>
- Van Gestel K, Stegers H, Von Witsch M, Šamay J, Baluška F, Verbelen JP** (2003) Immunological evidence for the presence of plant homologues of actin-related protein Arp3 in tobacco and maize: subcellular localization to actin-enriched pit fields and emerging root hairs. *Protoplasma* **222**: 45-52

Vartiainen MK, Machesky LM (2004) The WASP-Arp2/3 pathway: genetic insights. *Curr Opin Cell Biol* **16**: 174-181

Vidali L, Hepler PK (2001) Actin and pollen tube growth. *Protoplasma* **215**: 64-76

Vidali L, McKenna ST, Hepler PK (2001) Actin polymerization is essential for pollen tube growth. *Mol Biol Cell* **12**: 2534-2545

Vöchting H (1878) *Über Organbildung im Pflanzenreich*. Max Cohen, Tübingen

Vöchting H (1892) *Über Transplantation am Pflanzenkörper*. Verlag H. Laupp'sche Buchhandlung, Tübingen

Voigt B, Timmers AC, Samaj J, Müller J, Baluška F, Menzel D (2005) GFP-FABD2 fusion construct allows *in vivo* visualization of the dynamic actin cytoskeleton in all cells of *Arabidopsis* seedlings. *Eur J Cell Biol*. **84**: 595-608

Waller F, Riemann M, Nick P (2002) A role for actin-driven secretion in auxin-induced growth. *Protoplasma* **219**: 72-81

Went FW, Thimann KV (1937) *Phytohormones*. MacMilan, New York

Xu J, Scheres B (2005) Cell polarity: ROPing the ends together. *Curr Opin Plant Biol* **8**: 613-618

7. Appendix

7.1 Coding sequences of *AtFabd2* and *NtArp3*

7.1.1 *AtFabd2* gene

GATCCTCTTGAAAGAGCTGAATTGGTTCTCAGTCATGCAGAGAGAATGAA
CTGCAAGCGATACTTGACTGCAGAGGAGATCGTTGAAGGATCTTCAACTT
TGAATCTTGCCTTTGTGGCACAAATCTTCCATGAAAGGAATGGTCTAAAC
AAGGATGGTAAGTATGCATTTGCGGAGATGATGACCGAAGACGTAGAGAC
TTGTAGAGATGAACGATGCTACCGGCTATGGATCAACAGCCTCGGGATTG
ACAGTTATGTCAATAATGTATTTGAAGATGTTAGAAATGGATGGATTCTT
CTTGAGGTTCTTGACAAGGTCTCTCCAGTTCAGTCAACTGGAAGCATGC
TTCCAAACCACCGATTAAGATGCCGTTTAGAAAAGTAGAGAACTGCAATC
AAGTCATAAAGATCGGGAAACAGCTAAAATTCTCACTTGTAATGTAGCT
GGAAATGACATAGTTCAAGGGAATAAGAAGCTCATTCTTGGTCTCTTATG
GCAGTTGATGAGATTCCATATGCTCCAACCTCTCAAGAGTCTCAGATCTC
GGACACTAGGTAAAGAGATGACTGATGCAGATATCCTCAGCTGGGCCAAC
AGGAAAGTAAGAACAATGGGACGAAAATTGCAAATCGAGAGTTTCAAGGA
CAAGAGTCTATCGAGTGGGTTATTCTTCCTCAACCTTCTATGGGCGGTTG
AACCAAGAGTTGTGAACCTGGAATCTTGTCAACCAAGGGTCAAACAGATGAT
GAGAAGAGGTTGAATGCTACATACATAGTTAGTGTGCAAGAAAGCTCGG
TTGTTCCGTTTTCTTGTTACCTGAAGATATCGTGGAGGTGAATCAGAAGA
TGATCCTAATTTTAAACGGCAAGTATAATGTAAGTGGAGTCTTCAGAGACAT
TCACGGGAGAGTTCAGATTCGTGTCGTCAACTCAGAGCACCACAACGACGTG
CACCAGCACAGCCTCGTCCCCTGCCCCATCTGTACAGAAGAGGAGGAAG
TCTCCTCATTGAGCGGTGAAGTCACGAGCTTGGCCGTTGGTGATGCGGTT
TCTGAAATCACCACGGTCTCAGAGGAAGCATCCATCGAATAG

7.1.2 *NtArp3* gene

ATGGACCCTTCTACCTCTCGCCCAGCTGTAGTCATTGACAATGGAACCGGGTAT
ACAAAAATGGGTTTTGCTGGAAATGTTGAACCATCTTTCATACTGCCTACAGTT
GTCGCTGTTAACGAATCATTTATCAATCAGCCTCGAGCTTTGACTAAGAGCAGC
AACTTAGCTCAGTACAGTGCAGGAGTTATGGCTGATCTTGATTTCTTTATTGGG
GAAGAGGCATTGAGTAGATCTAAATCTAGTAGCACTTACAATCTTAGCTATCCT
ATTAACATGGACAGGTTGATAACTGGGATGCAATGGAGCGGTTCTGGCAGCAG
TGTGTATTCAATTATCTGCGCTGTGACCCTGAGGATCACTATTTTCTGTTGACT
GAAAGCCCTATGACTGCACCAGAGAACCGAGAATATACTGGTGAAATTATGTTT
GAGACTTTCAATGTTCCGGGACTTTATATAGCTGTGCAGCCGGTTCTTGCTCTG
GCAGCTGGGTACACAGCATCTAAGTGTGAGATGACTGGAGTCGTAGTGGATGTT
GGAGATGGTGCTACCCATGTTGTACCTGTTGCTGAAGGTTATGTTATTGGGAGT
AGCATTAAGTCAATCCCTGTTGCTGGGAAAGATGTTACTCTTTTCATTCAACAG
CTCATGAAGGAAAGGGGAGAGCATGTTCCAGCAGAGGATTCCTTAGAAGTAGCA
CGAAAAGTGAAGGAAATGTATTGCTATACTTGTCTGACATTGTGAAGGAGTCT
AATAAGCATGATAAAGAGCCAGGGAAGTACATCAAGCAATGGAGAGGTACAAAA
CCAAAGACAGGAGCACCATATTCATGTGATGTTGGCTATGAGCGATTTCTTGGT
CCTGAGGTTTTCTTCAATCCTGAGATCTATAATAGTGATTTTACGACCCCTTTA
CCTGATGTGATTGACAAATGTATCCAGTCTGCACCAATTGACACAAGAAGAGCT
TTATATAAGAATATTGTTCTATCCGGAGGATCAACCATGTTCAAAGACTTCCAT
AGAAGATTGCAGCGAGATCTCAAGAAGATTGTGGATGACCGTGTTCCTGCATCA
GATGCTCGGTTAGGTGGAAATGTCAAAGCACACCAGTTGAAGTGAATGTTGTC
AGCAATCCTATCCAGAGATATGCAGTTTGGTTTGGAGGTTCTGTACTAGCTTCA
ACTCCGGAATTTTTTGC GGCTTGCCATACAAAGACAGAATACGAGGAATATGGA
GCTAGCATATGCCGCACAAACCCTGTATTCAAGGGAATGTATTGA

7.2 Gateway® recombination reactions technology

The Gateway® technology (Invitrogen Corporation, Paisley, UK) uses the bacteriophage site-specific lambda recombination system to facilitate transfer of heterologous DNA sequences between vectors (Hartley et al., 2000). The components of the lambda recombination sites (*att* sites) are modified to improve the specificity and efficiency of the system (Bushman et al., 1985).

Two recombination reactions constitute the basis of this technology:

1. **BP reaction:** Facilitates recombination of an *attB* substrate (*attB*-PCR product) with an *attP* substrate (called “donor vector”) to create an *attL*-containing entry clone. This reaction is catalysed by BP Clonase™ II enzyme mix (Invitrogen).
2. **LR reaction:** Facilitates recombination of an *attL* substrate (called “entry clone”) with an *attR* substrate (called “destination vector”) to create an *attB*-containing expression clone. This reaction is catalysed by LR Clonase™ II enzyme mix (Invitrogen).

The presence of the *ccdB* gene within this system allows negative selection of the donor and destination vectors in *E. coli* following recombination and transformation. The CcdB protein interferes with *E. coli* DNA gyrase (Bernard and Couturier, 1992), thereby inhibiting growth of most *E. coli* strains. When recombination occurs (i.e. between an *attB*-PCR product and a donor vector or between an entry clone and a destination vector), the *ccdB* gene is replaced by the gene of interest. Cells that take up unreacted vectors carrying the *ccdB* gene or by-product molecules retaining the *ccdB* gene will fail to grow. This allows high-efficiency recovery of the desired clones.

For more information concerning the Gateway technology, refer to the manual “Gateway® Technology with Clonase™ II” (Invitrogen; <http://www.invitrogen.com>).

7.2.1 BP recombination reaction

To create *attL*-containing entry clones including the coding sequences of *AtFabd2* and *NtAtp3*, *attB*-PCR products were generated for the BP recombination reaction with the *attP*-containing donor vector pDONR/Zeo (Invitrogen) using the following primers. The underlined sites represent the *attB* sites.

attB1-FABD2 forward primer: 5'-GGGG ACA AGT TTG TAC AAA AAA GCA
GGC TTG GAT CCT CTT G-3'

attB2-FABD2 reverse primer: 5'-GGGG AC CAC TTT GTA CAA GAA AGC
TGG GTT CTA TTC GAT GGA TGC TTC CT-
3'

attB1-ARP3 forward primer: 5'-GGGG ACA AGT TTG TAC AAA AAA GCA
GGC TAT ATG GAC CCT TCT ACC TCT CG-
3'

attB2-ARP3 reverse primer: 5'-GGGG AC CAC TTT GTA CAA GAA AGC
TGG GTT TCA ATA CAT TCC CTT GAA TAC
AGG-3'

Following the BP reactions, chemi-competent *E. coli* (strain TOP 10, Invitrogen) were transformed by heat shock according to the manufacturer's protocol.

The zeocin resistance gene in pDONR/Zeo allowed selection of *E. coli* transformants using the antibiotic zeocin (Invitrogen). For selection, low salt LB agar plates (1% [w/v] tryptone, 0.5% [w/v] NaCl, 0.5% [w/v] yeast extract, 2% [w/v] agar) were used containing 50 mg/L zeocin.

7.2.2 LR recombination reaction

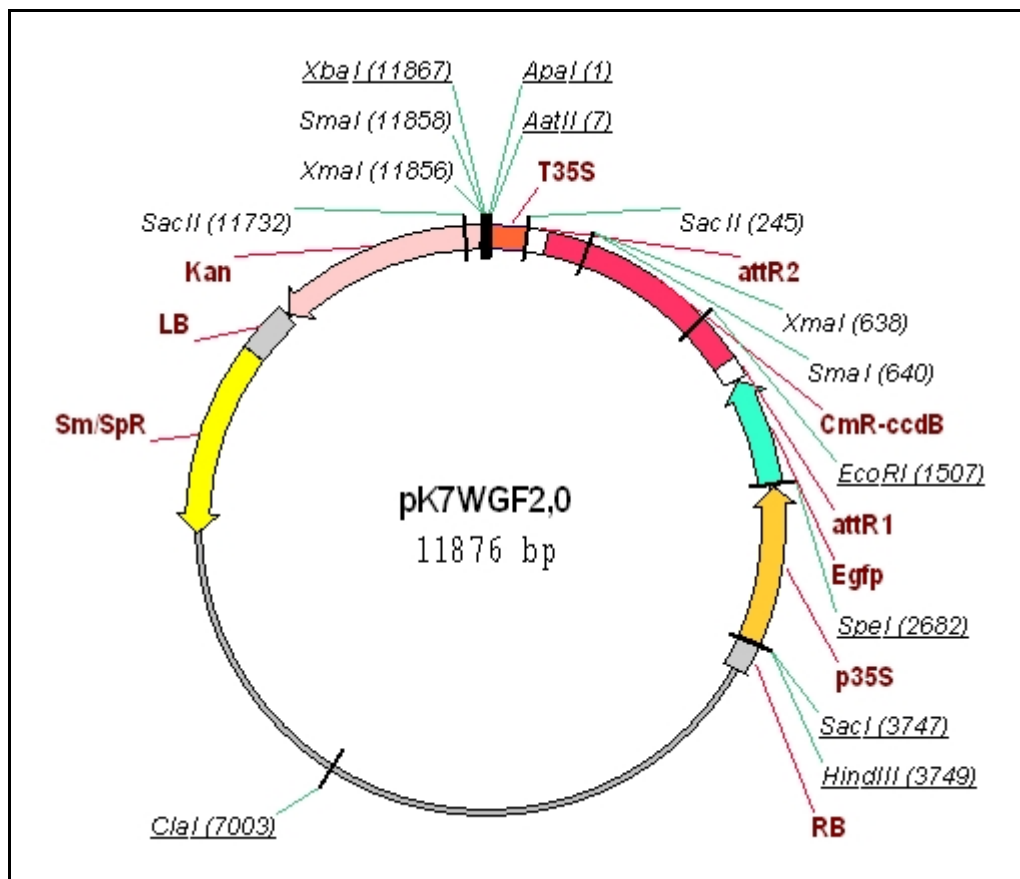
After generation of entry clones, the LR recombination reactions were performed to transfer the *AtFabd2* and *NtArp3* genes into the *attR*-containing destination vectors pK7WGF2 (Karimi et al., 2002; Karimi et al., 2005) and p2GWR7 (Campbell et al., 2002), respectively, to create *attB*-containing expression clones.

Following the LR reactions, chemi-competent *E. coli* (strain TOP 10, Invitrogen) were transformed by heat shock according to the manufacturer's protocol. For selection of expression clones, low salt LB agar plates were used containing 50 mg/L spectinomycin (pK7WGF2) or 100 mg/L ampicillin (p2GWR7).

7.3 Destination vectors

7.3.1 pK7WGF2

- binary vector for stable transformation of plants
- selection in *E.coli*: spectinomycin; selection in plants: kanamycin
- references: Karimi et al., 2002; Karimi et al., 2005

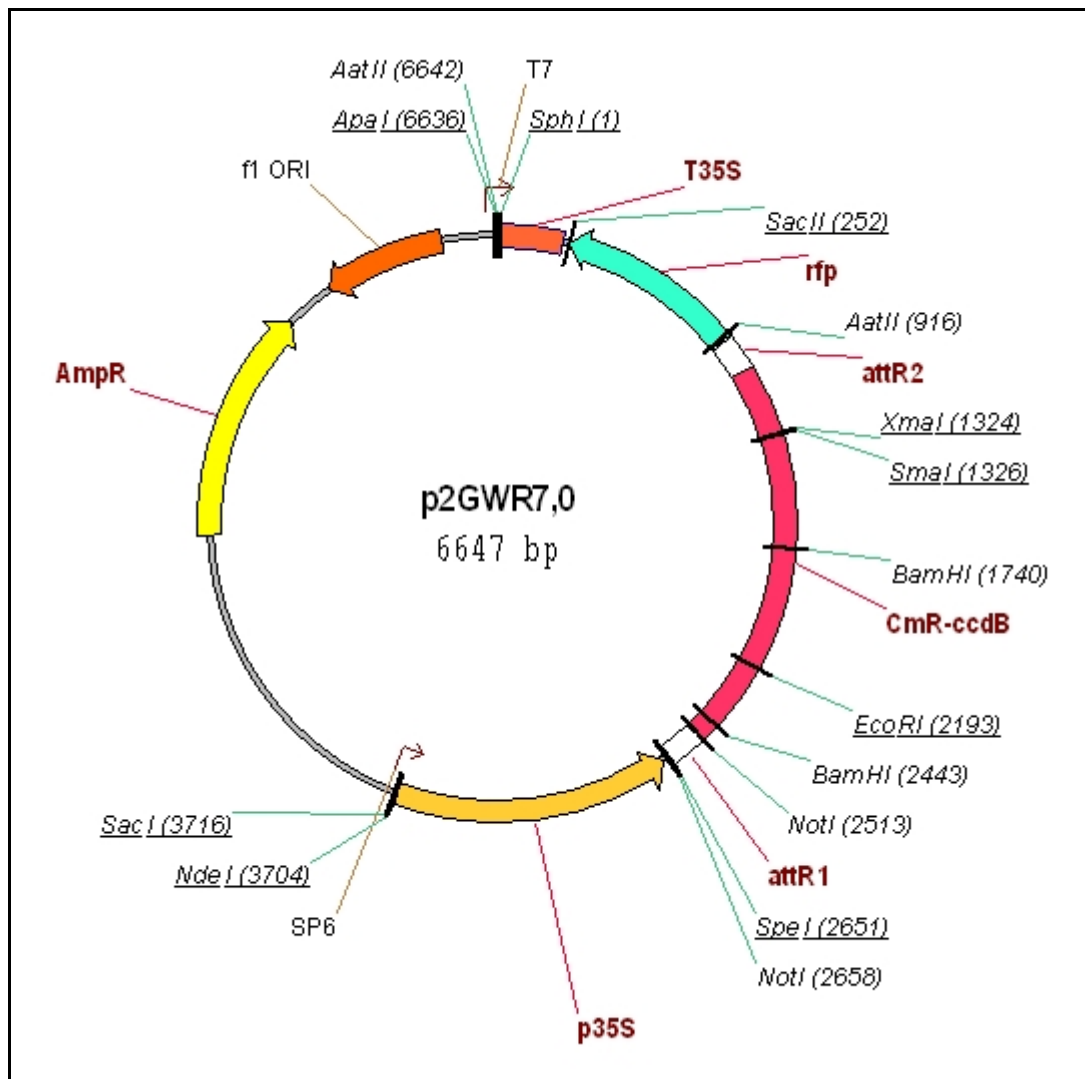


The following codes are used for naming the different elements of the construct:

- K:** kanamycin
- 7:** t35S terminator
- WG:** Gateway attR2, ccdB, attR1 orientation
- F:** GFP
- 2:** p35S promoter

7.3.2 p2GWR7

- high copy vector for transient transformation of plants
- selection in *E.coli*: ampicillin
- reference: Campell et al., 2002



The following codes are used for naming the different elements of the construct:

- 2:** p35S promoter
- GW:** Gateway attR1, ccdB, attR2 orientation
- R:** RFP
- 7:** t35S terminator

7.4 Swiss-Prot accession numbers of ARP3 homologues from diverse organisms

ARP3 homologue from	Swiss-Prot accession number (http://www.expasy.org)
<i>Acanthamoeba castellanii</i>	P53490
<i>Aedes aegypti</i> (Yellow fever mosquito).	Q16MG7
<i>Arabidopsis thaliana</i> (Thale cress)	Q9SAF1
<i>Aspergillus terreus</i>	Q0CW19
<i>Bos taurus</i> (Bovine)	P61157
<i>Caenorhabditis briggsae</i>	Q61WW9
<i>Caenorhabditis elegans</i>	Q9N4I0
<i>Cryptococcus neoformans</i>	Q55UI8
<i>Dictyostelium discoideum</i>	Q54QJ1
<i>Drosophila melanogaster</i> (Fruit fly)	P32392
<i>Fugu rubripes</i> (Japanese pufferfish)	O73723
<i>Homo sapiens</i> (Human)	Q9P1U1
<i>Mus musculus</i> (Mouse)	Q641P0
<i>Neurospora crassa</i>	P78712
<i>Oryza sativa</i> (Rice)	Q6K908
<i>Physcomitrella patens</i> (Moss)	Q0P7I1
<i>Saccharomyces cerevisiae</i> (Baker's yeast)	P47117
<i>Schizosaccharomyces pombe</i> (Fission yeast)	P32390
<i>Ustilago maydis</i> (Smut fungus)	Q4PFS9
<i>Xenopus laevis</i> (African clawed frog)	Q801P7

7.5 Preparation of DNA-coated gold particles for biolistic transformation

60 mg of gold particles (1.5–3.0 μm ; Sigma-Aldrich, Steinheim, Germany) were suspended in 50% (v/v) sterile glycerol by mixing on a platform vortexer (Bender & Hobein, Zurich, Switzerland).

Continuous agitation of the suspended gold particles was needed for uniform DNA precipitation onto gold particles maximising uniform sampling.

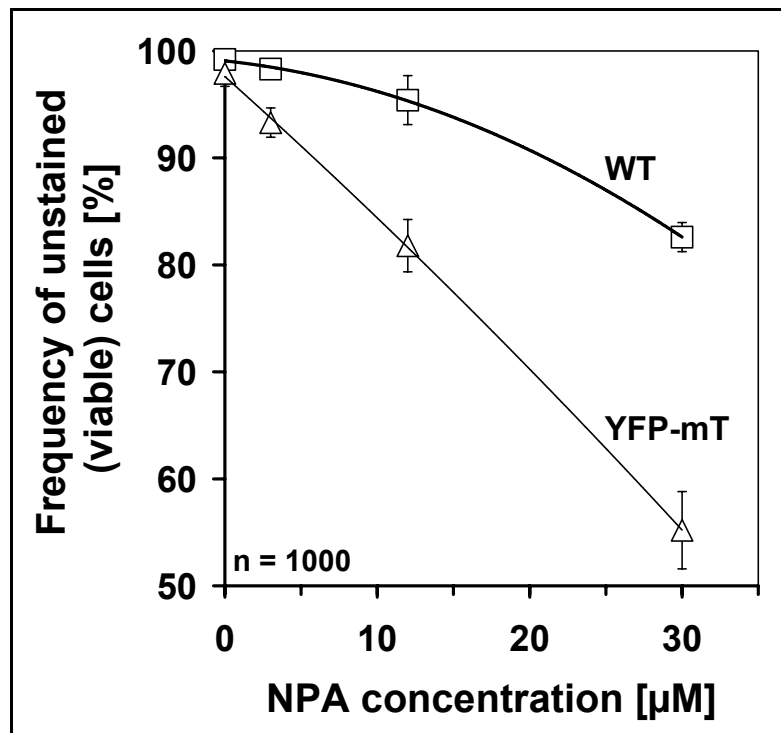
For each sample, 12.5 μL (0.75 mg) of gold suspension was removed to a 1.5-mL microcentrifuge tube.

While mixing vigorously, the following components were added successively: 1 μg of DNA, 12.5 μL of 2.5 M sterile CaCl_2 , and 5 μL of 0.1 M sterile spermidine (Roth, Karlsruhe, Germany).

Following supplementary mixing for 3 minutes, the DNA-coated gold particles were spun down briefly, and the supernatant was discarded. Subsequently, the gold particles were washed with 125 μL of absolute ethanol and resuspended in 37.5 μL of absolute ethanol.

DNA-coated gold particles were loaded onto the macrocarrier (BIO-RAD, Hercules, CA, USA) in 10 μL steps. Particle bombardment was performed immediately after total evaporation of the ethanol.

7.6 Effect of NPA on cell viability



The effect of NPA on the viability of non-transformed BY-2 cells (WT, *white squares*) versus cells overexpressing YFP-talin (YFP-mT, *white triangles*) at day 4 after inoculation was assayed by the Trypan Blue dye exclusion test (Phillips, 1973). For each individual sample, 1000 cells were scored. Error bars indicate SE.

Hiermit erkläre ich, dass ich die vorliegende Dissertation, abgesehen von der Benutzung der angegebenen Hilfsmittel, selbständig verfasst habe.

Alle Stellen, die gemäß Wortlaut oder Inhalt aus anderen Arbeiten entnommen sind, wurden durch Angabe der Quelle als Entlehnungen kenntlich gemacht.

Karlsruhe, im Dezember 2006

Jan Maisch

Publikation

Maisch J, Nick P (2007) Actin is involved in auxin-dependent patterning. *Plant Physiol*, in press.